DRUG DISCOVERY

Analysis of multi-target directed novel non-peptidic chalcone scaffold as potential malaria plasmodium proteases inhibitors

Sodeeq A Babalola[1*], **Muhammad Y Hayatuddeen**[2], **Idris A Yunusa**[2], **Hamza N Asmau**[2]

To Cite:
Babalola SA, Hayatuddeen MY, Yunusa IA, Asmau HN. Analysis of multi-target directed novel non-peptidic chalcone scaffold as potential malaria plasmodium proteases inhibitors. *Drug Discovery* 2023; 17: e25dd1935
doi: https://doi.org/10.54905/disssi.v17i39.e25dd1935

Author Affiliation:
[1]Chemistry Department, University of Minnesota, Twin cities, Minnesota, 55455, United States of America
[2]Department of Pharmaceutical Chemistry, Ahmadu Bello University, Zaira, Kaduna State, Nigeria

[*]**Corresponding author**
Chemistry Department, University of Minnesota, Twin cities, Minnesota, 55545,
USA
Email: wale.babalola91@gmail.com

Peer-Review History
Received: 26 March 2023
Reviewed & Revised: 30/March/2023 to 02/June/2023
Accepted: 06 June 2023
Published: 09 June 2023

Peer-Review Model
External peer-review was done through double-blind method.

Drug Discovery
pISSN 2278–540X; eISSN 2278–5396

DISCOVERY
SCIENTIFIC SOCIETY

ABSTRACT

Malaria remain an epidermic infectious disease that is ravaging the world most especially sub-Sahara Africa. Due to the prevalent of Plasmodium parasites that are resistant to first-line antimalarial drugs, it is urgently necessary to create new scaffolds and find strategies to overcome drug resistance. Chalcones are well-known, uncomplicated analogs that may be easily produced using a variety of techniques and are widely present in natural products. Utilizing in silico tools, we developed new antimalarial drugs from active synthetic and natural product fragments and then we assessed their pharmacokinetics and pharmacodynamic profiles as therapeutic molecules against the biological targets of the parasite that causes the deadly type of malaria. In this research, active fragments from prenylated and quinolinyl chalcones with known antimalarial characteristics were combined via molecular hybridization. Four enzymes that have been implicated to the spread of malaria are used as the biological targets in the docking simulation for the ligands (prenylated-quinolinyl chalcone hybrids). Receptor-ligand complexes were viewed using Discovery Studio Visualizer 2017 and Chimera. Web-based tools (Moftsoft, SwissADME, Admetlab and AdmetSAR 1 and 2) were utilized for drug-likeness and ADME prediction. The hybridized active segments created a brand-new scaffold with 169 new prenylated-quinolinyl chalcones. Post-docking studies found significant interactions between the drugs and the used targets. At least 25 of the compounds exhibit high affinities for the targets (-9.4 to -7.5 kcal/mol-1). The selected compounds had interesting ADME and drug-like properties. The compounds were qualified as possible antimalarial drugs due to their realistic pharmacokinetic and pharmacodynamic characteristics as well as their prospective antimalarial activity.

Keywords: Prenylated chalcones, Quinolinyl chalcones, SAR, Docking simulation, Molecular hybridization, Plasmodium falciparum, Rule of three, Rule of five, ADMET, SUB1, Plasmepsin II, Falcipain 2, Falcipain 3, Drug-likeness, Malaria, Antimalaria agents.

1. INTRODUCTION

Malaria continues to be one of the most common infections, with 247 million cases worldwide resulting in more than 619,000 deaths yearly. Children and pregnant women are the populations most vulnerable to this sickness (WHO, 2023). The first-line antimalarial drugs now in use continue to be ineffective against Plasmodium falciparum, the most dangerous malaria parasite (Kashyap et al., 2017). International researchers are always seeking novel approaches to combat the new parasite strain. The discovery and development of novel antimalarial medications over the past several years has enhanced awareness of the need to eradicate and prevent malaria (Burrows et al., 2017; White et al., 2016; Phyo et al., 2016). The papain-family cysteine proteases falcipain-2 (FP-2) and falcipain-3 (FP-3) are known to catalyze the proteolysis of host hemoglobin in Plasmodium falciparum, a step required for the development of erythrocytic parasites (White et al., 2016).

A group of proteases in the parasite's acidic digestive vacuole break down hemoglobin. Plasmapsin, an aspartic protease present in the vacuole, attacks the hemoglobin molecule first before falcipain, a cysteine protease, separates the large pieces into minute peptides (Kerr et al., 2009). Since intact hemoglobin cannot be broken down by falcipain without first being denatured, the first cleavage by plasmepsin is essential for hemoglobin degradation. It is thought that this cleavage causes the haemoglobin molecule to disassemble, effectively facilitating subsequent proteolysis.

SUB1, a serine protease that resembles subtilisin, has been shown to promote egress (Asojo et al., 2003). Minutes before egress, the still intracellular merozoite releases a SUB1 from specialized secretory organelles known as exonemes as a result of a calcium and cGMP-dependent signal (Withers-Martinez et al., 2014; Yeoh et al., 2007; Collins et al., 2013). One of the most abundant merozoite surface and parasitophorous vacuole resident soluble proteins that are proteolytically changed by SUB1 upon release into the vacuole lumen is SERA6, a potential cysteine protease implicated in egress and invasion (Withers-Martinez et al., 2014; Yeoh et al., 2007; Collins et al., 2013; Agarwal et al., 2012; Koussis et al., 2009; Ruecker et al., 2012).

When SUB1 discharge or catalytic activity is pharmaceutically suppressed, released merozoites are prevented from exiting and/or their capacity to infiltrate the host is lowered (Withers-Martinez et al., 2014; Collins et al., 2013). A new class of antimalarial therapies is urgently needed to combat the parasite's rising drug resistance and drugs that target SUB1 activity should have potential as a new class of antimalarial therapeutics (Thomas et al., 2018). New ideas are always being searched for to stop the proliferation of the parasite resistant types. The discovery and development of novel antimalarial drugs over the past several years has enhanced awareness of the need to eradicate and prevent malaria (Burrows et al., 2017; White et al., 2014; Phyo et al., 2016).

Researchers are under pressure to provide new treatments and preventative measures for malaria infections since the Plasmodium parasite is growing more and more resistant to widely used antimalarial drugs like chloroquine and artemisinin and its derivatives. Because there isn't currently a licensed malaria vaccine available to develop immunity, chemotherapy continues to be the best alternative (Siezen et al., 1997). Novel antimalarial strategies include enhancing therapies utilizing already-approved drugs (such as artemisinin combination therapy), repurposing drugs, developing analogs of already-approved drugs and testing and using chemosensitizers treatment techniques (drug-resistance reversers) (WHO, 2013; Schlitzer, 2008; Biamonte et al., 2013; Klein, 2013; Muregi et al., 2011).

But another approach has recently attracted a lot of interest in the field of modern medicinal chemistry. In order to create a single hybrid entity with a dual mode of action, two physiologically active molecules (pharmacophores) must be combined. In comparison to the parent medications, these new hybrid compounds have the potential to increase efficacy, improve safety, be more affordable and minimize the tendency to provoke resistance (Walsh and Bell, 2009; Muregi and Ishih, 2010; Meunier, 2012). The notion of hybridization has been shown to be a useful tool for creating novel antimalarial active ingredients (Menezes et al., 2002).

Chalcones provide a variety of therapeutic benefits, such as antiplasmodial action. They are essentially secondary metabolites found in plants that belong to the flavonoid family and serve as important building blocks for both individual flavonoids and isoflavonoids. Due to their many pharmacological effects, particularly their anti-malarial efficacy, they have undergone substantial research. Chalcones may also be easily created using the economical Claisen-Schmidt condensation of acetophenones with variably substituted benzaldehydes, yielding a variety of unique potential analogues with strong pharmacological properties.

The anti-malarial activity of chalcone was first reported after an *in-vitro* assessment of an oxygenated chalcone, "licochalcone A," derived from Chinese licorice, as an antimalarial drug against chloroquine sensitive and chloroquine resistant Plasmodium strains. In addition, a large number of possible licochalcone A analogues with various patterns of substitution have been identified as having powerful anti-malarial action. Several chemists have been drawn to the straightforward design and clear synthesis of chalcones in their quest to develop novel analogues of this peculiar framework for treating numerous infectious illnesses, including malaria.

Disease selection, target identification and validation, lead finding and optimization, preclinical and clinical trials and drug discovery and development are all extremely time-consuming and expensive processes (Sinha et al., 2019). The number of novel molecular entities (NMEs) that the US. Food and Drug Administration (FDA) have authorized has clearly increased in recent years with the advent of *in-silico* technologies (Guan et al., 2019). Many drug ideas still fall short of becoming actual medications, though. The two main factors that contribute to therapeutic failure are ineffectiveness and safety (Siramshetty et al., 2016); therefore, chemical characteristics like absorption, distribution, metabolism, excretion and toxicity (ADMET) are crucial at every stage of drug discovery and development. Finding effective compounds with improved ADMET characteristics is therefore important (Guan et al., 2019).

In this study, structure-activity relationship (SAR) guided design of eight series of the novel scaffold of chalcone by extensive SAR survey of active quinolinyl chalcones and prenylated chalcones from the literature, molecular hybridization of the pharmacophoric fragments resulted to 169 novel prenylated-quinolinyl chalcone hybrids. Molecular docking and pharmacokinetics studies were also conducted. We have previously report the synthesis and antimalarial of prenylated acetophenone fragment 8 (Yahya et al., 2023).

2. METHODS

Structure-activity relationships and hybridization concept of the fragments

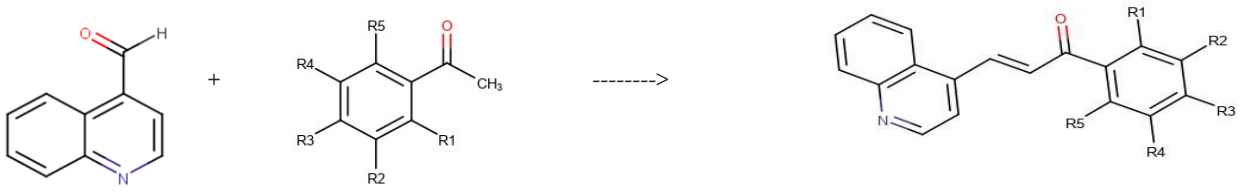

Frag a + Frag 1-21 --------> 1-21

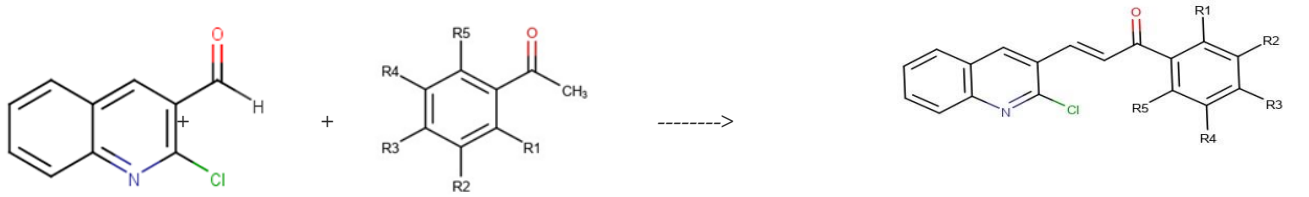

Frag b + Frag 1-21 --------> 22-42

Frag c + Frag 1-21 --------> 43-63

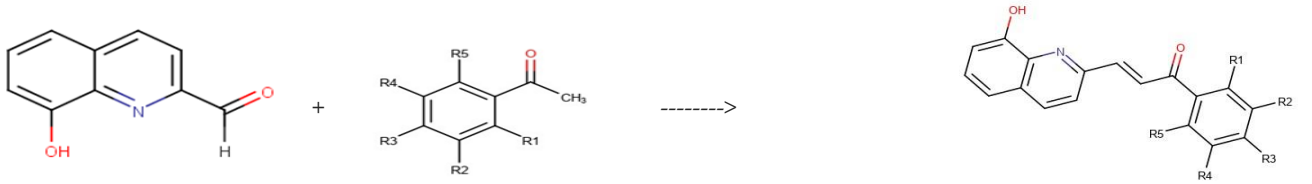

Frag d + Frag 121 --------> 64-84

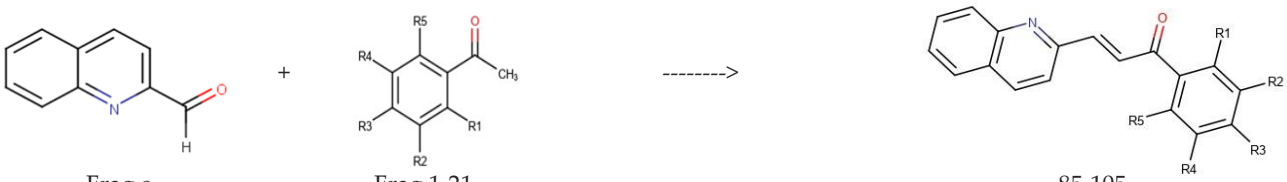

Frag e + Frag 1-21 --------> 85-105

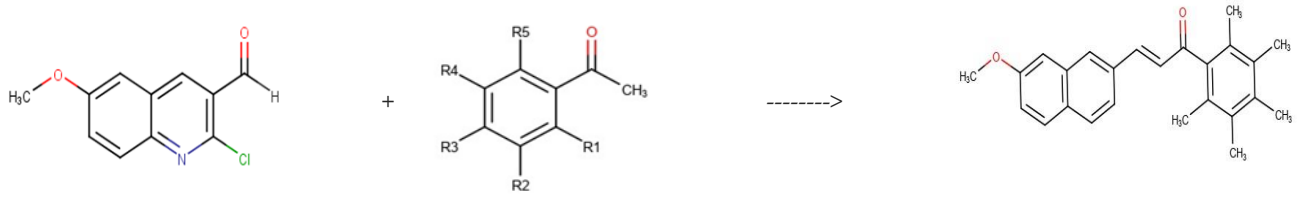

Frag f + Frag 1-21 --------> 106-126

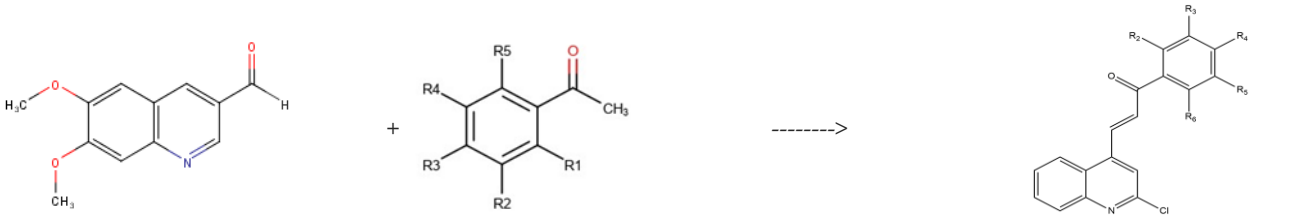

Frag g + Frag 1-21 --------> 127-148

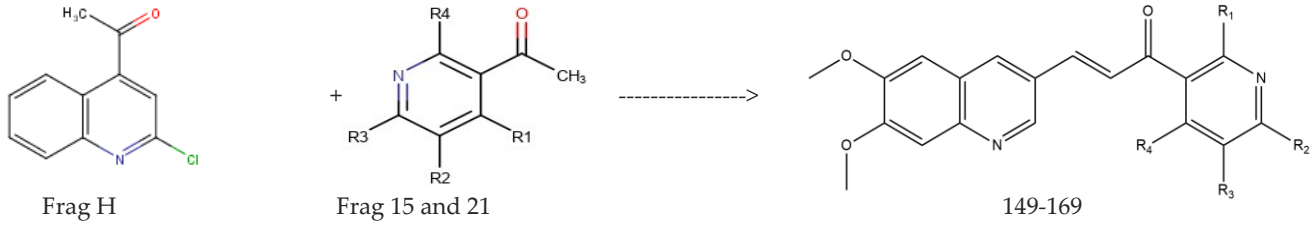

Frag H + Frag 15 and 21 ----------> 149-169

Prenylated acetophenone fragments substitution pattern

	R2	R3	R4	R5	R6
1	OH	Prenyl	OH	H	H
2	H	Prenyl	CH_3O	H	OH
3	H	Isoprenyl	OH	H	CH_3O
4	OH	Prenyl	H	Prenyl	OH
5	OH	Prenyl	OH	H	CH_3O
6	OCH_3	H	OH	Isopropyl	OH
7	H	3`-OH-2-methylbutenyl	OH	H	OH
8	H	Prenyl	OH	H	OH
9	H	Prenyl	OH	2Prenyl	O
10	Cl	Isoprenyl	H	Cl	H
11	OH	Prenyl	Cl	Cl	CH_3O
12	H	Isoprenyl	OH	CH_3O	CH_3O
13	F	Prenyl	F	H	OH
14	OH	Prenyl	CH_3O	H	CH_3O
15	OH	Prenyl	OH	N	OCH_3
16	H	Prenyl	CH_3O	CH_3O	H
17	CH_3O	Prenyl	OH	H	H
18	H	Prenyl	OH	H	H
19	OH	Prenyl	H	H	OH
20	CH_3O	Prenyl	OH	H	OH
21	OH	Prenyl	OH	N	OH

Protein Crystal Structure and Ligand Collection

Four malarial biological targets were used for the docking study viz; Three-dimensional (3D) crystal structures of the proteins; *Pf* Plasmepsin II, *Pf* Falcipain 2, *Pf* Falcipain 3 and *Pf* SUB1. The 3D crystal structures of the targets were retrieved from Protein Data Bank, Plasmepsin II (ILF3) (Phyo et al., 2016), Falcipain 2 (3BPF) (Mullard, 2018), Falcipain 3 (3BWK) (Jhoti et al., 2013) and *Pf* SUB1

(4LVO) (Daina and Zoete, 2016), respectively. Chloroquine was used as the reference drugs and it structure was retrieved from PubMed and Protein Data Bank (PDB).

Molecular Docking Using Autodock Vina

Using bash commands in the Cygwin run time environment, the Autodock Vina script was used to simulate docking. In this investigation, the binding sites of Pf Plasmepsin II, Pf Falcipain 2, Pf Falcipain 3 and Pf SUB1 were simulated using 169 prenylated-quinolinyl chalcone compounds. Flexible docking mode was used during the docking process, which automatically generates conformations for each input ligand. To evaluate the ligand's interaction with the receptor, the created ligand poses were put through a series of hierarchical filters.

This method rewards positive hydrogen bonding, hydrophobic and metal-ligation interactions while penalizing steric conflicts. The binding energies of the ligands were graded using Excel when the simulation was finished. Each ligand pose (conformation) was viewed in UCSF chimera 1.11.2 (www.cgl.ucsf.edu/chimera); the most favorable complexes formed were viewed in the discovery studio software (https://discover.3ds.com/discovery- studio-visualizer-download) wherein various interactions between the ligands and the receptors were elucidated in a two-dimensional (2D) format (Babalola et al., 2022).

Drug-Likeness, *In Silico* Pharmacokinetics and Toxicity Studies

Following a rule of three (RO3) evaluations, the fragments were hybridized (Guan et al., 2019). Selected compounds with best affinity were further examined using drug-likeness characteristics and in silico pharmacokinetics and toxicity studies were conducted using the ADMETlab 2.0 and Protox-II web servers (https://admetmesh.scbdd.com) and tox-new.charite.de, respectively. The pharmacokinetic features of absorption, distribution, metabolism and excretion (ADME) as well as specific drug-likeness factors were assessed using the ADMETlab 2.0. On web servers for Protox-II and ADMETlab 2.0, the toxicity investigations were carried out. A two-way analysis of variance (ANOVA) with replication, a residual error test and Tukey's multiple comparison test were used to statistically examine the data (Babalola et al., 2022).

3. RESULTS AND DISCUSSION

Fragment Screening

Rule of Three (RO3) has been useful in ensuring that fragment libraries really do consist of compounds with active fragment-like properties (Clark and Pickett, 2000). The parameters of 'Rule of Three' are such that a molecule with molecular weight ≤300, the number of hydrogen bond donors is ≤3, the number of hydrogen bond acceptors is ≤3, ClogP is ≤3, NROT (≤3) and PSA (≤60) would be an active fragment. Any fragment that passes these rules on the average could be useful when constructing fragment libraries for efficient lead discovery (Clark and Pickett, 2000). The RO3 was applied to the fragment library to assess whether our derived active fragments possess the parameters to exhibit active fragment-like properties. All the fragments passed the RO3 as in Table 1, fragments 5, 6, 7, 11, 13, 15, 16 and 20 passes the RO3 only on the average.

Hybrid Screening

Eight series of a novel scaffold comprising of 169 hybrids resulted from the hybridization of the screened fragments as listed above. The best twenty-five (25) hybrids with high affinity for at least two (2) biological targets were selected from the docking score ranking (unpublished). Nineteen of these compounds have higher affinities for three receptors (Falcipain 2, Falcipain 3 and SUB1) compared to the respective receptors' natural inhibitors.

Table 1 Rule of three (RO3) evaluation of the fragments

Fragment	MW≤300 ($gmol^{-}$)	MlogP≤3	HBA≤3	HBD≤3	NROT≤3	PSA≤60 $Å^2$
Frag-a	157.17	1.14	2	0	1	29.96
Frag-b	191.61	1.70	2	0	1	29.96
Frag-c	251.67	1.06	4	0	3	48.42
Frag-d	173.17	0.53	3	1	1	50.19
Frag-e	157.17	1.14	2	0	1	29.96
Frag-f	221.64	1.37	3	0	1	39.19
Frag g	190.63	3.03	1	0	1	17.07
Frag 1	220.26	1.89	3	2	3	57.53
Frag 2	234.29	2.15	3	1	4	46.53

Frag 3	234.29	2.15	3	1	4	46.53
Frag 4	288.38	3.05	3	2	5	57.53
Frag 5	250.29	1.57	4	2	4	66.76
Frag 6	252.31	1.65	4	2	5	66.76
Frag 7	236.26	1.04	4	3	4	77.76
Frag 8	220.26	1.89	3	2	3	57.53
Frag 9	356.50	3.16	3	0	7	51.21
Frag 10	257.16	4.22	1	0	3	17.07
Frag 11	303.18	3.19	3	1	4	46.53
Frag 12	264.32	1.82	4	1	5	55.76
Frag 13	240.25	3.30	4	1	3	37.30
Frag 14	264.32	1.82	4	1	5	55.76
Frag 15	251.28	0.90	5	1	4	79.65
Frag 16	264.32	1.82	4	1	5	55.76
Frag 17	234.29	2.15	3	1	4	46.53
Frag 18	204.26	2.50	2	1	3	37.30
Frag 19	220.26	1.89	3	2	3	57.53
Frag 20	250.29	1.57	4	2	4	66.76
Frag 21	237.25	0.62	5	3	3	90.65

MW: Molecular weight
MlogP: Partition Co-efficient
HBA: Hydrogen bond donor
HBD: Hydrogen bond acceptor
NORT: Number of rotatable bonds.
PSA: Polar surface area

Table 2 Physicochemical properties of the selected hybrid compounds

Cmpds	MW	nHD	nHA	Rot	nRing	nHET	TPSA(Å)	logS	logP	logD
2a	373.170	1	4	6	3	4	59.420	-5.969	5.648	4.015
4a	427.210	2	4	7	3	4	70.420	-4.354	7.159	4.154
4b	460.180	2	3	7	3	4	57.530	-5.475	8.100	4.727
4e	427.210	2	4	7	3	4	70.420	-4.579	7.130	4.200
7c	449.180	3	7	7	3	7	109.110	-5.131	4.218	3.303
8b	393.110	2	3	5	3	5	70.420	-5.175	5.598	4.056
8d	375.150	3	5	5	3	5	90.650	-3.867	5.117	3.701
8f	422.130	2	4	6	3	5	66.760	-6.053	6.478	4.233
10e	395.080	0	2	6	3	4	29.960	-7.519	6.321	4.394
11d	457.080	2	5	6	3	7	79.650	-5.365	6.452	3.98
11e	441.090	1	4	6	3	6	59.420	-6.461	6.535	4.126
13a	379.140	1	3	5	3	5	50.190	-6.244	5.895	4.115
13b	412.100	1	4	5	3	5	37.300	-7.409	6.919	4.677
13d	395.130	2	6	5	3	6	70.420	-4.876	5.549	3.806
13e	379.140	1	5	5	3	5	50.190	-6.587	5.833	4.193
13f	443.110	1	6	6	3	7	59.420	-7.234	5.888	4.153
15d	406.150	3	7	6	3	7	112.770	-3.429	4.680	3.102
16d	403.180	1	5	7	3	5	68.650	-5.199	5.108	3.869
18d	359.150	2	4	5	3	4	70.420	-4.009	4.907	3.812
19a	359.150	2	4	5	3	4	70.420	-4.138	5.715	3.678
21a	389.160	2	5	6	3	5	79.650	-4.250	5.356	3.703
21d	392.140	4	7	5	3	7	123.770	-3.361	4.567	2.111

MW; Molecular Weight
logP: Partition co-efficient
AA: Aromatic atoms
HBD: Hydrogen bond donor
NORT: Number of rotatable bonds
MR: Molar refractivity
HBA: Hydrogen bond acceptor
RO5: Rule of five
HA: Heavy atoms
logS: Aqeous solubility
PSA: Polar surface area

All the selected chalcones exhibit drug-like physicochemical properties, having a molecular weight (MW) of less than 600 gmol^{-}, less than 12 hydrogen bond acceptors (nHA) and less than 7 hydrogen bond donor (nHD). The designed chalcones had ess than 6

rings (nRing), fewer than 11 rotatable bonds (nRot) and less than 15 heteroatoms (nHet). Only compounds 8d and 21d showed substantial water solubility, despite the fact that all of the chosen chalcones have less than 140 topological polar surface area (TPSA).

Also, most of the compounds had logP greater than 5 mol/L except for compounds 7c, 15d, 18d and 21d with logP equal to 4.218 mol/L, 4.680 mol/L, 4.907 mol/L and 4.567 mol/L respectively. Since the likelihood of successful oral absorption and interactions with molecular targets tend to rise as hydrophobicity increases, it is crucial for drug molecules to have this property. However, when hydrophobicity increases, the likelihood of effective renal or biliary drug excretion from the body decreases. The biotransformation of hydrophobic drug molecules into more hydrophilic ones, often known as metabolism, is a crucial step in the process of eliminating medicines from the body.

As a result, compounds with strong hydrophobicity and hydrophilicity balance typically have better ADME profiles. These compounds also met Veber et al., (2002) optimal conditions for bioavailability. All of the compounds fulfilled Ghose's total number of atoms and all of them are in accordance with Lipinski rule of five. All the compounds exhibit less than 5.0 threshold score for lipophilicity at physiologic pH $logD_{7.4}$.

Table 3 Medicinal Chemistry Friendliness

Compds	QED	SA score	Fsp3	MCE-18	PAINS	BMS	Alarm NMR	Chelator rule
2°	0.289	2.619	0.20	13	0	0	3	0
4°	0.413	3.011	0.25	19	0	0	1	0
4b	0.168	3.063	0.21	21	0	0	2	0
4e	0.228	3.15	0.21	21	0	0	2	1
7c	0.343	2.69	0.36	19	1	3	2	0
8b	0.252	2.69	0.13	19	0	0	3	0
8d	0.340	2.79	0.13	19	0	0	3	1
8f	0.229	2.75	0.16	20	0	0	5	0
10e	0.241	2.87	0.08	18	0	0	1	0
11d	0.247	3.02	0.20	21	0	0	2	1
11e	0.263	2.86	0.17	20	0	0	2	0
13°	0.355	2.82	0.13	19	0	0	2	0
13b	0.232	2.90	0.13	20	0	0	2	0
13d	0.558	3.10	0.17	19	0	0	1	1
13e	0.355	2.83	0.13	19	0	0	2	0
13f	0.210	2.95	0.17	21	0	0	4	0
15d	0.341	2.94	0.24	20	0	0	2	1
16b	0.194	2.57	0.20	19	0	0	3	0
16d	0.327	2.67	0.20	19	0	0	3	1
18d	0.380	2.63	0.13	18	0	0	3	1
19a	0.380	2.63	0.13	18	0	0	2	0
19d	0.384	2.81	0.13	19	0	0	0	1
21a	0.351	3.05	0.14	19	0	0	4	0
21d	0.295	3.14	0.14	20	1	0	3	1

The Quantitative estimation of drug-likeness (QED) of the selected hybrids falls between ranges 0.168 to 0.413. These scores are much lower than 0.67 thresholds for attractive compounds. All the compounds fall within the easy to synthesize scores (1-4) for their synthetic accessibility (*SA*) score. The selected hybrids exhibited less than 0.42 fraction of sp^3 hybridized carbon suggesting that they have low to moderate flexibility. The medicinal chemistry evolution 2018 (MCE-18) scores of all the compounds are less than 45 with scores ranging from 13 to 21 indicating that the compounds are simple structured molecules with old scaffolds and a low degree of 3D complexity according to results (Table 3).

Among the selected hybrid compounds, only 7c and 21d gave an alert for Pan-assay interference (PAINS) substructure and also hybrid 7c gave three alerts for Bristol-Myers Squibb (BMS) rule. All the selected hybrids gave alerts ranging between 1-5 for alarm NMR rule indicating that the hybrid consist in their structure reactive centers, consequently can possibly serve as irreversible covalent inhibitors of the corresponding biological targets. Hybrid 4e and every other hybrid that consist of fragment d gave one alert each for Chelator rule.

Chemical compounds known as pan-assay interference chemicals (PAINS) frequently produce results that are false-positive (false hits) in high-throughput screening assays. Instead of directly impacting intended targets, they frequently react in a non-specific manner with many biological targets. Since the PAINS compounds are bad hits, they are frequently removed from compound libraries. Compounds that have the potential to be reactive or promiscuous are also found using the alert NMR rule. A reliable indication of potential phase I and phase II metabolic reactions of substances can be found in the reactivity warnings from alarm NMR.

The Bristol-Myers Squibb (BMS) rule is used to screen out harmful reactive substances and chemicals that have the potential to be toxic. Chelators such as crown-ether-like compounds are especially undesirable in drug discovery inputs and are rejected because of their potential to act as ionophores in addition to their poor druggability. However, these filters, it cannot distinguish between bad or innocent suspects this includes covalent inhibitors.

During the time and resource-consuming processes of drug discovery and development, enormous number of molecular compounds is evaluated using diverse parameters in order to determine the selection of which chemicals to synthetize, test and promote, with the sole aim of identifying those with the best likelihood of becoming an effective medicine for the patients. The molecules must show high biological activity together with low toxicity. Chemical absorption, distribution, metabolism, excretion (ADME), play key roles in drug discovery and development. A good drug candidate should not only have effective efficacy against the therapeutic target, but also show teeming ADME properties at a therapeutic dose (Trott and Olson, 2010).

Table 4 Absorption

Compd	Caco-2	MDCK	HIA	P-gp inhibitor	P-gp-substrate	F 30%	F 20%
2a	-4.94	21×10^{-5}	0.1	0.6	0.2	0.1	0.1
4a	-4.92	2.7×10^{-5}	0.1	0.9	0.2	0.7	0.9
4b	-4.91	2.1×10^{-5}	0.1	0.9	0.1	0.9	0.2
4e	-4.99	2.1×10^{-5}	0.1	0.8	0.1	0.6	0.3
7c	-4.96	1.5×10^{-5}	0.1	0.1	0.1	0.1	0.1
8b	-4.89	1.7×10^{-5}	0.1	0.4	0.1	0.9	0.1
8d	-4.98	1.5×10^{-5}	0.1	0.3	0.1	0.3	0.1
8f	-490	1.5×10^{-5}	0.1	0.7	0.1	0.1	0.7
10e	-4.82	8.8×10^{-5}	0.1	0.8	0.2	0.8	0.3
11d	-4.87	19×10^{-5}	0.1	0.9	0.1	0.1	0.1
11e	-4.77	1.3×10^{-5}	0.1	0.9	0.1	0.6	0.1
13a	-4.94	2.1×10^{-5}	0.1	0.7	0.1	0.7	0.1
13b	-4.92	1.8×10^{-5}	0.1	0.7	0.6	0.6	0.1
13d	-5.01	3.4×10^{-5}	0.1	0.9	0.1	0.6	0.1
13e	-4.90	1.7×10^{-5}	0.1	0.9	0.1	0.6	0.1
13f	-4.94	1.6×10^{-5}	0.1	0.9	0.1	0.1	0.1
15d	-4.88	2.9×10^{-5}	0.1	0.9	0.1	0.1	0.1
16b	-4.77	1.2×10^{-5}	0.1	0.9	0.1	0.1	0.1
16d	-4.81	1.3×10^{-5}	0.1	0.6	0.1	0.1	0.1
18d	-4.85	1.4×10^{-5}	0.1	0.1	0.1	0.1	0.3
19a	-4.85	1.8×10^{-5}	0.1	0.1	0.1	0.1	0.6
19d	-4.95	1.5×10^{-5}	0.1	0.1	0.1	0.5	0.9
21a	-4.88	1.9×10^{-5}	0.1	0.1	0.1	0.1	0.1

The predictive human colon adenocarcinoma cell lines (Caco-2) *in-vivo* drug permeability values of all the compounds range between -5.01 log cm/s for compound 13d and -4.77 log cm/s for compounds 16b and 11e respectively, which were greater than -5.15 log cm/s earmarked for compounds with proper Caco-2 *in-vivo* drug permeability. This indicates that all the selected hybrids would be permeable *in-vivo* according to the results (Table 4).

All the selected hybrids also indicated a high passive apparent permeability coefficient (P_{app}) in the predictive Madin–Darby Canine Kidney cells (MDCK) *in-vitro* model for permeability screening. Values ranging between 1.2×10^{-5} for hybrid compound 16b which and 21×10^{-5} for compound 2a. Most of the compounds fall within the range of low to medium permeability except for compound 16b which value is categorized as highly passive permeability. The selected hybrid compounds demonstrated plausible results in the human intestinal absorption (HIA) predictive model. All the compounds had HIA+ scores of 0.1 indicating that they are non-HIA+ i.e their human intestinal absorption far exceeds >30% absorbance.

Hybrid compounds 7c, 8b, 8d, 18d, 19a, 19b and 21a indicated strong inhibitory potential of P-glycoprotein with scores of 0.1, 0.4, 0.3, 0.1, 0.1, 0.1 and 0.1 respectively. All other selected hybrids compounds indicated poor inhibitory potential of P-glycoproteins. According to Table 4 all the selected hybrids may be metabolized by P-glycoproteins, exception is for compound 13b which indicated moderate affinity as P-gp substrate. P-gp is thought to act as a barrier to intestinal drug absorption because it is found in large quantities on the villus tip of enterocytes' apical membrane, where it extrudes substrate from inside the cell back into the intestine's lumen. The role of P-gp in drug absorption has been demonstrated in a variety of preclinical investigations employing *in-vitro* cellular systems and MDR1 knockout mice that lack ABCB1 and thus do not express P-gp (Babalola et al., 2022; Robertson et al., 2012).

A common conclusion from these investigations is that intestinal P-gp blockage or absence increases the systemic availability of medicines that are P-gp substrates, which may result in toxicity or improved efficacy. This does not, however, imply that all P-gp substrates will have decreased oral absorption when a P-gp inhibitor is present. Numerous drugs that are P-gp substrates have a good bioavailability due to intestinal P-gp saturation at clinically relevant doses. Vinblastine, digoxin, ritonavir, etoposide, indinavir and verapamil are a few examples of P-gp substrates with excellent oral availability (Babalola et al., 2022; Robertson et al., 2012).

It is therefore common to overestimate the significance of intestinal P-gp inhibition as a contributor to drug-drug interactions (DDIs). Only drugs administered in small dosages (50 mg) or with slow dissolution and/or membrane diffusion rates are likely to exhibit drug interactions brought on by P-gp inhibition in the gut that are clinically significant. There are exceptions for some drugs that are taken at high doses (over 50 mg), however, these drugs are either big (>800 Da) or produced in formulations that take a long time to dissolve. Cyclosporine, paclitaxel and saquinavir hard-gel capsules are a few examples of such drugs (Babalola et al., 2022; Robertson et al., 2012).

In contrast to intestinal P-gp inhibition, which is seldom the cause of clinically significant DDIs, induction of P-gp has been demonstrated to decrease the bioavailability of P-gp substrates, leading to clinically significant DDI (Babalola et al., 2022; Robertson et al., 2012). All the designed compounds have shown a good balance between P-gp inhibition and substrate tendencies which may lead to less DDIs and toxicity.

The 30% and 20% oral bioavailability prediction suggests that F30% of selected hybrid compounds 4a, 4b, 4e, 8b, 8f, 10e, 8b, 8f, 10e, 11e, 13a, 13b, 13d, 13e, 19a and 19d score is categorized with low to moderate oral bioavailability. On the other hand, selected hybrid compounds 4a, 8f, 19a and 19d had low oral bioavailability for F20% oral bioavailability.

Table 5 Distribution

Compd	PPB (%)	Volume distribution (L/kg)	BBB	F_u (%)
2a	100.00	0.931	0.1	0.805
4a	97.55	4.513	0.1	3.835
4b	104.958	2.453	0.3	1.109
4e	101.27	1.744	0.1	1.54
7c	98.047	0.486	0.1	1.403
8b	102.11	0.380	0.1	0.36
8d	100.448	0.601	0.1	0.738
8f	101.199	0.395	0.1	0.491
10e	101.88	0.378	0.1	0.258
11d	101.28	1.557	0.1	0.766

11e	101.80	1.070	0.1	0.555
13°	100.60	1.230	0.1	0.692
13b	102.71	0.635	0.1	0.365
13d	100.078	2.191	0.1	0.713
13e	100.901	0.825	0.1	0.483
13f	102.591	0.539	0.1	0.439
15d	99.782	0.562	0.1	0.684
16b	98.348	0.553	0.1	0.984
16d	94.190	0.452	0.1	1.527
18d	100.012	0.466	0.1	0.561
19a	100.808	0.789	0.1	0.882
19d	101.202	0.488	0.1	0.574
21a	100.685	0.567	0.1	0.815

The plasma protein binding of the selected hybrid compounds was found to be between 104.958% and 94.190 which is greater than 90% maximum earmarked for proper plasma protein binding (PPB) according to results (Table 5). The plasma protein binding of the compounds are notwithstanding within the admissible range as many approved drugs were found to have greater than 90% plasma protein binding. It has been noticed that many clinically successful drugs exhibit high PPB. This is in fact the truth as evidenced by the statistics of drugs approved by the United States Food and Drug Administration (FDA).

Nearly 30% of the 260 marketed drugs that the US Food and Drug Administration (FDA) had approved before 2003 have PPB levels above 95%. This range is often regarded as having significant drug binding to plasma proteins. Additionally, 5% had PPB > 99%, which is regarded as having a very high PPB. The PPB of 45% of recently authorized medications is > 95%, while the PPB of 24% is > 99%, according to statistics on PPBs for pharmaceuticals approved by the US FDA from 2003 to 2013. These findings show that compounds with PPB > 99% can still be valuable drugs (Babalola et al., 2022; Mansoor and Mahabadi, 2021; Liu et al., 2014)

The volume distribution (Vd) of the selected hybrid compounds were found to be between 0.38 L/kg to 4.513 L/kg according to results (Table 6). These results fall in the proper Vd is in the range of 0.04-20 L/kg. An individual drug's propensity to either stay in the plasma or disperse to different tissue compartments is represented by the volume distribution (Vd), a pharmacokinetic parameter. It establishes a connection between the overall amount of drug in the body and its plasma concentration at a particular moment. This parameter is affected by physiological plasma volume, physiological tissue volume, PPB and tissue binding.

The distribution process is the movement of the medicine between the intravascular (blood/plasma) and extravascular (intracellular & extracellular) compartments of the body. In every area of the body, a drug coexists in balance between a protein-bound and free form. Drugs in the blood will ultimately be metabolized by the liver and kidneys and evacuated from the body (Babalola et al., 2022; Liu et al., 2014).

A greater dose of a medicine is necessary to reach a given plasma concentration for a substance with a high Vd because such compounds are more likely to leave the plasma and enter the extravascular compartments of the body. More distribution to other tissues is associated with high Vd. On the other hand, a medication with a low Vd has a tendency to stay in the plasma, requiring a lower dosage to reach a given plasma concentration. Less distribution to other tissues when Vd is low. The proper Vd is in the range of 0.04-20 L/kg.

Acid-base character and lipophilicity have considerable influence on a compound's volume distribution. Throughout the body, drugs may have a tendency to bind proteins until they find equilibrium between the bound and unbound phases. A drug may tend to bind macromolecules within or outside the plasma depending on its charge at physiological pH. On phospholipid membranes, negatively charged phospholipid head groups interact strongly with basic (alkaline) molecules. The degree of this binding is also influenced by the drug's general lipophilicity.

When compared to acidic molecules, basic molecules often leave the systemic circulation with a greater volume distribution (Vd). Compared to neutral or basic compounds, acidic molecules have a stronger affinity for albumin molecules at lower lipophilicity. As a result, compared to more basic molecules, acidic drugs are more likely to bind albumin and stay in the plasma, resulting in a reduced volume distribution (Vd) (Babalola et al., 2022; Mansoor and Mahabadi, 2021).

All the selected hybrids compounds have been predicted to be Blood Brain Barrier (BBB) with scores of 0.1. However, the fraction unbound F_u of all the selected compounds is less than 5% for proper F_u. F_u is determined as free drug concentration divided by the total drug concentration. Free drug concentration is the concentration of the unbound drug or compound. The free drug

hypothesis is a widely accepted pharmacological norm that postulates that, in the absence of transporters, the free drug concentration is the same on both sides of the biological membrane at a steady-state and the species that exerts pharmacological activity, such as *in-vivo* efficacy and toxicity, is the free drug or unbound concentration at the site of action.

For the first part of the hypothesis, this may be true for the designed chalcones considering their high passive permeability and possible fast rate of permeation which can fasten the rate of reaching equilibrium across membranes. However, for the second part of the hypothesis, there are some exceptions that could apply to designed chalcones as do other drugs as follows. Chalcone Bridge is a reactive center comprising both nucleophilic and electrophilic characters. This enables the moiety to interact irreversibly with the biological target forming covalent bonds with amino residues of the target in addition to reversible interactions with the therapeutic target. Therefore, the activity of chalcones is dependent on the cumulative concentration of irreversibly bound chalcones or possible metabolite to the target.

The free drug concentration will always determine the initial binding kinetics of the chalcones to the target or the site of action, but the subsequent time course of receptor occupancy and the pharmacodynamics events that the chalcones triggers do not follow the time course of free drug concentration. This is because the efficacy of the chalcones will depend on the inactivation of the biological target and the time taken for the body to resynthesize the biological target and not on the free drug concentration in plasma.

Table 6 Metabolism

Compd	CYP1A2		CYP2C19		CYP2C9		CYP2D6		CYP3A4	
	Subst.	Inhib.	Subst.	Inhib.	Subst.	Inhib.	Subst.	Inhib.	Subst.	Inhib.
2°	0.1	0.7	0.1	0.7	0.7	0.9	0.9	0.8	0.3	0.6
4°	0.3	0.7	0.2	0.7	0.6	0.8	0.6	0.6	0.2	0.6
4b	0.4	0.6	0.1	0.9	0.9	0.9	0.7	0.5	0.2	0.2
4e	0.2	0.7	0.1	0.9	0.6	0.6	0.6	0.6	0.3	0.3
7c	0.5	0.7	0.9	0.1	0.6	0.9	0.4	0.8	0.6	0.3
8b	0.8	0.3	0.8	0.1	0.9	0.9	0.6	0.6	0.5	0.4
8d	0.9	0.3	0.9	0.1	0.7	0.7	0.7	0.7	0.3	0.5
8f	0.4	0.7	0.1	0.9	0.9	0.9	0.7	0.7	0.4	0.2
10e	0.3	0.9	0.1	0.9	0.9	0.9	0.6	0.6	0.3	0.6
11d	0.4	0.6	0.2	0.6	0.9	0.9	0.7	0.4	0.2	0.3
11e	0.3	0.6	0.1	0.6	0.9	0.9	0.7	0.4	0.3	0.4
13a	0.3	0.9	0.1	0.9	0.9	0.9	0.6	0.6	0.4	0.6
13b	0.6	0.3	0.9	0.1	0.9	0.9	0.4	0.6	0.4	0.3
13d	0.4	0.6	0.1	0.9	0.9	0.7	0.6	0.9	0.2	0.2
13e	0.4	0.9	0.1	0.9	0.9	0.9	0.6	0.5	0.4	0.3
13f	0.4	0.7	0.1	0.9	0.9	0.9	0.6	0.5	0.6	0.2
15d	0.9	0.7	0.4	0.9	0.9	0.9	0.6	0.9	0.3	0.5
16b	0.5	0.7	0.3	0.9	0.9	0.9	0.6	0.3	0.3	0.5
16d	0.4	0.6	0.1	0.6	0.9	0.9	0.4	0.6	0.7	0.2
18d	0.3	0.9	0.1	0.9	0.6	0.9	0.9	0.6	0.3	0.6
19a	0.3	0.9	0.1	0.9	0.9	0.9	0.7	0.9	0.3	0.7
19d	0.2	0.1	0.9	0.1	0.7	0.9	0.7	0.7	0.1	0.5
21a	0.1	0.9	0.3	0.1	0.7	0.9	0.5	0.7	0.3	0.1

Table 6 represents the prediction of metabolism of the selected hybrid compounds by the CYP450 metabolizing enzymes. As indicated in the results, each of the hybrid compounds may be a strong inhibitor and/or substrate of particular CYP450 metabolizing enzymes. Except for compound 8b, 8d and 15d which show no substrate affinity to CYP1A2, all other selected hybrids indicated strong to moderate substrate potential of CYP1A2 with scores ranging between 0.1 and 0.5 suggesting that they are susceptible to metabolism by CYP1A2. Compounds 8b, 8d, 13b and 19d indicated strong inhibitory potential of CYP1A2 while

compounds 4b, 11d, 11e, 13d and 16d indicated moderate to weak CYP1A2. All other compounds are with scores suggesting they are poor inhibitors of the enzymes according to results (Table 6).

All the compounds with exception of compounds 7c, 8b, 8d, 13b and 19d are predicted to have high substrate affinity for enzyme CYP2C19 according to results (Table 6). Among the selected hybrid compounds, only compound 7c, 8b, 8d, 11d, 13b, 19d and 21a indicated potent inhibitory potential against CYP2C19. All other compounds indicated poor inhibitory potential against CYP2C19 metabolizing enzyme. All the compounds indicated moderate to weak potential as substrates and inhibitors of CYP2C9 and CYP2D6 suggesting that they may not be metabolized by the metabolizing enzyme as suggested by the results (Table 6). All the selected compounds indicated strong to moderate substrate and inhibitory potential of CYP3A4 metabolizing enzyme suggesting that they have balance between their inhibitory and substrate potential as indicated (Table 6).

Table 7 Excretion

Compd	Clearance (ml/min/kg)	Half-life ($T_{1/2}$)
2a	8.714	0.388
4a	12.434	0.174
4b	9.251	0.046
4e	13.143	0.164
7c	11.414	0.369
8b	8.395	0.234
8d	11.025	0.717
8f	8.567	0.222
10e	3.490	0.050
11d	7.918	0.060
11e	5.054	0.036
13a	4.729	0.043
13b	5.965	0.046
13d	9.569	0.265
13e	5.244	0.046
13f	6.613	0.054
15d	7.488	0.091
16b	6.907	0.149
16d	8.358	0.367
18d	9.968	0.584
19a	7.504	0.139
19d	11.699	0.363
21a	4.616	0.626

The results of the clearance and half-lives of the selected hybrids are presented (Table 7). Among the compounds, only compounds 10e, 13a and 21a have less than 5 ml/min/kg suggesting that they have low clearance. All other compounds have their clearance within the range of 5-15 ml/min/kg which categorized them as compounds with moderate clearance. Except for compounds 8d and 21a which scores (0.717 and 0.626) suggests that their half-lives maybe less or equal to or less than three hours. All other compounds have their scores greater than three hours according to the results (Table 7).

Half-life ($T_{1/2}$) refers to the time required for the plasma concentration of a drug to decrease by 50%. The $T_{1/2}$ of the initial phase (alpha-phase $T_{1/2}$) represents the distribution of the drug and the $T_{1/2}$ of the second phase (beta-phase $T_{1/2}$) represents the elimination of the drug from the body. The $T_{1/2}$ results reported herein are the beta-phase $T_{1/2}$.

Table 8 Binding affinity analysis of the selected compounds for *Pf* Plasmepsin II

Cpds	*Pf* Plasmepsin II				
	BE (ΔG)	Interacting Residue	H-bond	HI	Types of HI
2a	-8.9	ASP214, 1LE32, MET15, PHE16, SER79, VAL78	1 (SER79 2.92Å)	7	Van der Waals, Pi-Anion, Alkyl, Pi-Alkyl
4a	-8.6	ASP214, GLY216, ILE32, ILE300, LEU131, LEU292, MET75, PHE294, TYR77, TYR192, SER79, VAL78	1 (ASP214 3.08Å),1 (TYR192 2.89Å)	12	van der Waals, Pi-Donor H-bond, Pi-Sigma, Alkyl, Pi-Alkyl
4b	-8.5	ALA117,ASP214,ILE14,ILE32,ILE123,MET15,SER118,TYR77	1 (SER118 2.69Å)	11	van der Waals, Pi-Anion, Pi-Sigma, Alkyl, Pi-Alkyl
4d	-9.2	ASP214, GLY216, ILE32, ILE123, ILE290, PHE294, TYR77, TYR192, VAL78	1 (GLY216 1.87Å)	9	van der Waals, Pi-Anion, Pi-Sigma, Alkyl, Pi-Alkyl
4e	-9.1	ASP214, GLY216, ILE32, ILE123, ILE290, PHE294, TYR192, VAL78	1 (GLY216 1.92Å), 1 (TYR192 2.74Å)	8	van der Waals, Pi-Anion, Pi-Sigma, Alkyl, Pi-Alkyl
7c	-7.5	ASP214, MET15, SER79, TYR192, VAL78	1 (MET15 2.31Å), 1 (SER79 2.71Å), 2 (TYR192 3.02Å,3.15Å)	4	van der Waals, Pi-Donor H-bond, Pi-Sigma, Alkyl, Pi-Anion
8b	-8.1	GLY216, ILE32, ILE300, MET15, TYR77, TYR192, VAL78	1 (GLY216 2.85Å), 1 (TYR192 3.03Å)	6	van der Waals, Pi-Donor H-bond, Pi-Sigma, Pi-Sulfur, Alkyl, Pi-Alkyl
8d	-9.4	ASP214, ILE32, MET15, PHE16, SER79, TYR192, VAL78	2 (ASP214 2.33Å,2.23Å), 1 (SER79 1.93Å)	8	van der Waals, Pi-Pi T-shaped, Alkyl, Pi-Alkyl
8f	-8.2	ASP214, ILE300, LEU292, PHE29, SER79, THR217, TYR77, TYR192, VAL78	1 (ASP214 2.26Å), 1 (THR217 2.97Å), 1 (TYR192 2.69Å)	9	van der Waals, Pi-Donor H-bond, Pi-Sigma, Pi-Pi Stacked, Pi-Pi T-Shaped, Alkyl, Pi-Alkyl
10e	-8.9	GLY216, ILE32, ILE123, ILE212, ILE300, LEU292, PHE294, TYR77, TYR192, VAL78	1 (GLY216 1.95Å)	15	van der Waals, Pi-Donor H-bond, Pi-Sigma, Alkyl, Pi-Alkyl
11d	-9.4	GLY216, ILE32, ILE123, ILE290, ILE300, LEU292, MET15, PHE294, THR217, TYR77, TYR192, VAL78	1 (GLY216 1.94Å 2.81Å), 1 (THR217)	13	van der Waals, Pi-Sigma, Alkyl, Pi-Alkyl
11e	-9.2	GLY216, ILE32, ILE123, ILE290, ILE300, LEU292, PHE294, THR217, TYR77, TYR192, VAL78	1(GLY216 1.91Å), 1(THR217 2.79Å)	11	van der Waals, Pi-Sigma, Alkyl, Pi-Alkyl
13a	-7.7	ASP214, ILE32, ILE123, SER79, SER218, TYR77, VAL78	1(SER79 2.94Å), 1(SER218 3.12Å)	6	van der Waals, Pi-Anions, Alkyl, Pi-Alkyl
13b	-8.8	LEU292, PHE294, SER79, TYR77, TYR192	0	5	van der Waals, Alkyl, Pi-Alkyl
13d	-9.2	ASP214, GLY216, ILE32, ILE290, LEU292, MET15, THR217, VAL78	1 (GLY216 1.89Å), 1 (THR217 3.14Å)	9	Halogen (F), Pi-Sigma, Alkyl, Pi-Alkyl
13e	-9.4	ASP214, GLY216, ILE32, ILE123, ILE290, LEU292, MET15, THR217, TYR77, TYR192, VAL78	1 (GLY214 3.05Å), 1 (THR 2.02Å)	11	Halogen (F), Pi-Sigma, Alkyl, Pi-Alkyl
13f	-8.2	ASP214, ILE300, LEU292, SER79, THR217, VAL78	1(THR217 3.11Å)	8	Halogen (F), Pi-Donor H-bond, Alkyl, Pi-Alkyl
15d	-8.7	ASP214, GLY216, ILE32, ILE123, ILE290, THR217, TYR77, VAL78	1 (ASP214 2.83Å), 1 (THR217 1.84Å), 1 (GLY216 1.91Å)	6	Pi-Sima, Alkyl, Pi-Alkyl
16b	-8	ASP214, GLY216, LEU292, MET15, PHE294, TYR192, VAL78, THR217, TYR192	1 (ASP214 2.62Å),1 (THR217 2.17Å)	11	C-H,Unfavorable Acceptor-Acceptor, Alkyl, Pi-Alkyl
16d	-8.2	ASP214, GLY216, ILE32, ILE123,	2 (GLY216 1.97Å,1.81Å)	7	van der Waals, C-H, Pi-Anion,

		PHE294, TYR77, TYR192, VAL78			Pi-Sigma, Alkyl, Pi-Alkyl
18d	-9.3	ASP214, ILE32, PHE16, MET15, THR217, VAL78	2 (ASP214 2.28Å, 2.39Å), 1 (THR217 2.22Å)	7	van der Waals, Alkyl, Pi-Alkyl
19a	-8.4	ASP214, ILE32, MET15, PHE16, SER79, VAL78	2(SER79 2.28Å, 2.80Å)	7	van der Waals, C-H, Pi-Anion, Pi-Sigma, Alkyl, Pi-Alkyl
19d	-8.8	ASP34, ASP214, GLY216, ILE14, ILE212, ILE300, MET15	1 (ASP34 2.32Å), 2 (GLY216 2.10Å, 2.82Å), 1 (ILE14 3.00Å), 1 (SER218 2.38Å)	10	Pi-Anion, Pi-Sulfur, Alkyl, Pi-Alkyl
21a	-8.0	ASP214, GLY36, ILE32, ILE123, MET15, SER79, SER218, PHE120, TYR77, VAL78	1 (ASP214 2.28Å), 1 (SER79 2.80Å)	9	C-H, Unfavorable Donor-Donor, Pi-Donor H-bond, Pi-Pi Stacked, Alkyl, Pi-Alkyl
21d	-8.0	ASP214, GLY216, ILE14, ILE32, MET15, SER79, SER218, THR217	2 (ASP214 2.38Å, 2.40Å), 1 (GLY216 2.21Å), 1 (ILE14 3.08Å), 1 (SER79 3.05Å), 1 (SER218 3.16Å), 1 (THR217 2.16Å)	3	Pi-Sulfur, Alkyl

BE: Binding Energy H-bond: Hydrogen bond HI: Hydrophobic Interacting

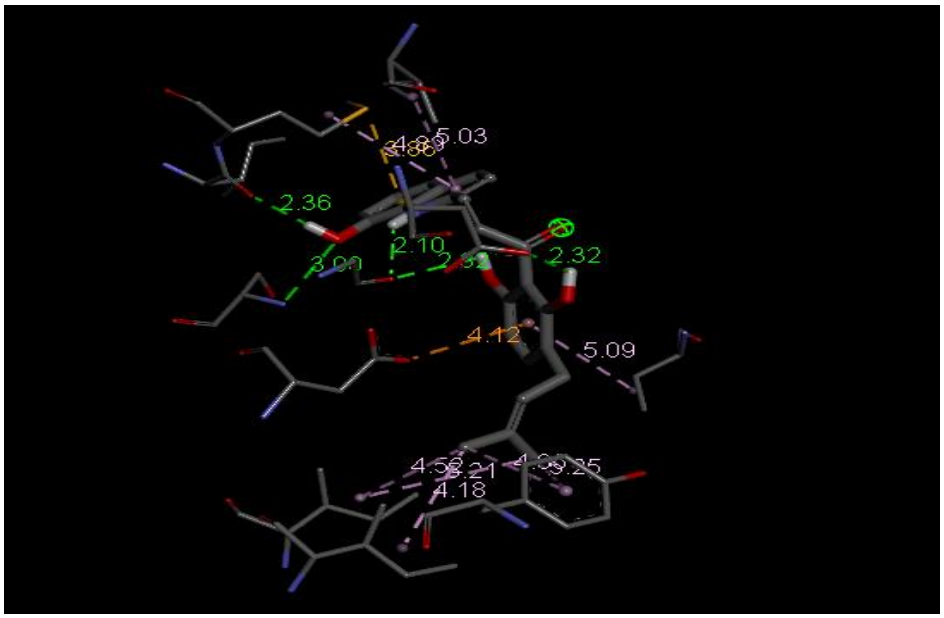

(a)

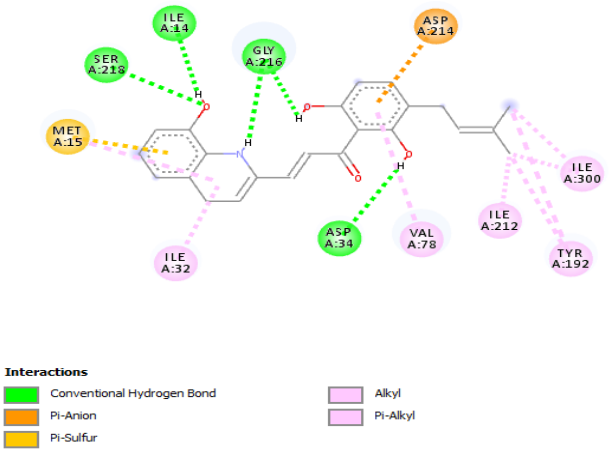

(b)

Figure 1 Binding interaction of 19d with Plasmepsin II in 3D (a), and 2D (b)

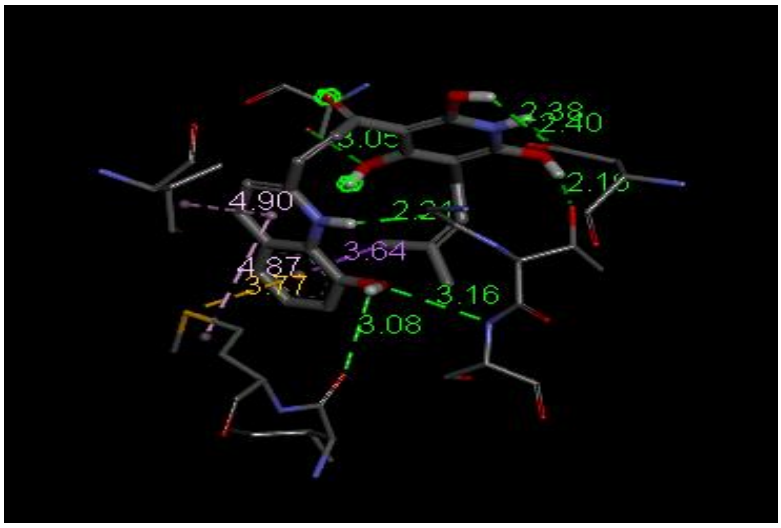

(a)

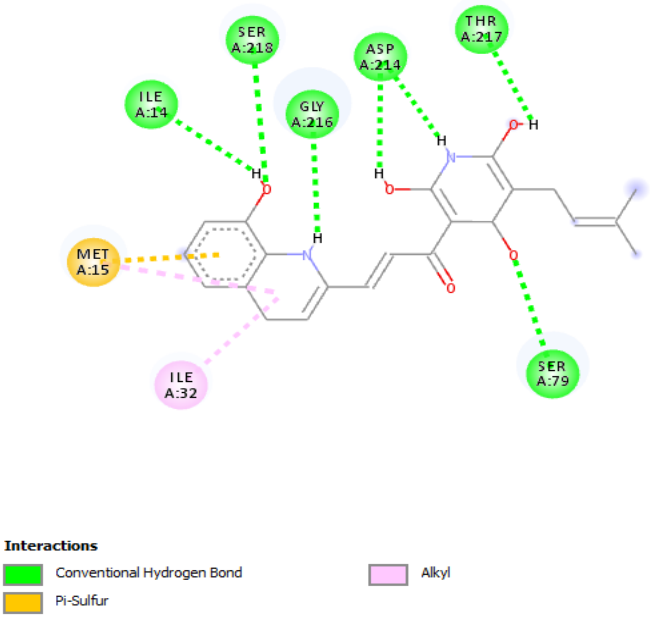

(b)

Figure 2 Binding interaction of 21d with Plasmepsin II in 3D (a) and 2D (b)

Table 9 Binding affinity analysis of the selected compounds for *Pf* Falcipain 2

Cpds	*Pf* Falcipain 2				
	BE (ΔG)	Interacting residues	H-bond	Hydophobic interaction	Types of HI
2a	-6.8	ALA175, ASN173, CYS42, GLY82, HIS174, LEU84, TYR78	—	7	van der Waals, C-H bond, Pi-Pi T-shaped, Amide-Pi Stacked, Alkyl, Pi-Alkyl
4a	-7.6	ALA175, CYS42, ILE85, LEU84	___	6	van der Waals, C-H bond, Pi-Sulfur, Alkyl, Pi-Alkyl
4b	-7.3	ALA175, CYS42, ILE85, LEU84, TYR78	____	9	van der Waals, Pi-Sulfur, Pi-Pi T-shaped, Alkyl, Pi-Alkyl
4d	-7.5	ALA175, CYS42, GLN36,	1 (GLN36 2.53Å), 1	12	C-H bond, Pi-Sulfur, Alkyl, Pi-

		GLY82, GLY83, ILE85, LEU84, TRP43, TYR78	(GLY83 1.98Å)		Alkyl
4e	-7.4	ALA175, ASN173, CYS42, ILE85, HIS174, LEU84, TYR78	____	8	van der Waals, C-H bond, Pi-Sulfur, Pi-Pi T-shaped, Alkyl, Pi-Alkyl
7c	-7.5	ALA175, ASN173, CYS42, HIS174, LEU84, TRP43	1 (HIS174 2.76Å)	7	C-H bond, Amide-Pi Stacked, Pi-Alkyl
8b	-7.4	CYS42, ILE85, LEU84, TYR78	____	8	van der Waals, Pi-Sulfur, Pi-Pi T-shaped, Alkyl, Pi-Alkyl
8d	-7.7	ASN77, CYS42, GLY83, HIS174, ILE85, LEU84, TYR78	1 (ASN77 2.39Å), 1 (HIS174 3.05Å)	8	Unfavorable Donor-Donor, Pi-Sulfur, Pi-Pi T-shaped, Alkyl, Pi-Alkyl
8f	-7.1	ALA175, CYS39, CYS42, ILE85, LEU84	____	6	van der Waals, Amide-Pi Stacked, Alkyl, Pi-Alkyl
10e	-7.7	ALA175, ASN173, CYS42, HIS174, ILE85, LEU84, TRP43	1 (ASN173 2.02Å)	11	van der Waals, Halogen (Cl, Br, I), Pi-Pi Stacked, Amide-Pi Stacked, Alkyl
11d	-7.6	ALA175, ASN173, CYS42, GLY83, ILE85, HIS174, LEU84, TRP206	1 (ASN173 1.99Å), 1 (GLY83 2.13Å)	8	van der Waals, C-H bond, Unfavorable Acceptor-aAcceptor, Pi-Pi Stacked, Amide-Pi Stacked, Alkyl
11e	-7.7	ALA175, ASN173, CYS42, GLY82, GLY83, ILE85, HIS174, LEU84, LEU172	1 (ASN173 2.08Å), 1 (GLY83 2.40Å)	10	C-H bond, Pi-Pi Stacked, Amide-Pi Stacked, Alkyl, Pi-Alkyl
13a	-7.4	ALA175, CYS42, ILE85, HIS174, LEU84	1 (ALA175 2.77Å)	7	C-H bond,Halogen(F), Pi-Sulfur, Alkyl, Pi-Alkyl
13b	-7.7	CYS42, ILE85, HIS174, LEU84, TYR78	1 (HIS174 2.98Å)	8	van der Waals, Halogen (F), Pi-Sulfur, Pi-Pi T-shaped, Alkyl, Pi-Alkyl
13d	-7.8	ALA175, ASN173, CYS42, GLY82, GLY83, HIS174, ILE85, LEU84, LEU172	2 (ASN173 1.99Å,2.30Å), 1 (GLY83 2.44Å)	10	C-H bond, Halogen(F), Pi-Pi Stacked, Alkyl, Pi-Alkyl
13e	-7.7	ALA175, ASN173, CYS42, GLY82, GLY83, ILE85, HIS174, LEU84, LEU172, SER149, TRP206	1 (ASN173 1.86Å), 1 (GLY83 2.16Å)	12	C-H bond, Halogen(F), Pi-Pi Stacked, Amide-Pi Stacked, Alkyl, Pi-Alkyl
13f	-7.4	ALA175, CYS42, GLY82, GLY83, ILE85, LEU84, LEU172	___	9	van der Waals, C-H bonds, Halogen (F), Alkyl, Pi-Alkyl
15d	-7.5	ASN77, CYS42, GLY82, GLY83, ILE85, LEU84, LYS76, TYR78	1 (ASN77 2.19Å), 1 (LYS 2.70), 1 (GLY83 2.52)	7	C-H bond, Pi-Sulfur, Pi-Pi T-shaped, Alkyl, Pi-Alkyl
16b	-7.1	ALA175, CYS42, GLY83, ILE85, LEU84	2 (GLY83 2.62Å, 2.70Å)	6	C-H bond, Alkyl, Pi-Alkyl
16d	-7.3	ALA175, ASN173, CYS42, GLY82, GLY83, HIS174, ILE85, LEU84, TRP206	1 (ASN173 1.98Å), 1 (GLY 2.15Å)	9	C-H bond, Unfavorable Acceptor-Acceptor, Pi-Pi Stacked, Alkyl, Pi-Alkyl
18d	-7.6	ALA175, ASN173, CYS42, GLY82, GLY83, ILE85, HIS174, LEU84	1 (ASN173 1.85Å), 1 (GLY83 2.43Å)	9	C-H bond, Pi-Pi Stacked, Amide-Pi Stacked, Alkyl, Pi-Alkyl
19a	-7.3	ALA175, CYS42, GLY40,	1 (GLY83 2.15Å)	8	van der Waals, C-H bond, Pi-

		GLY82, GLY83, ILE85, HIS174, LEU84, TRP43			Sulfur, Alkyl
19d	-7.7	ALA175, ASN173, CYS42, GLY83, ILE85, HIS174, LEU84	1 (ASN173 2.34), 1 (GLY83 2.42Å)	9	van der Waals, C-H bond, Pi-Pi Stacked, Alkyl, Pi-Alkyl
21a	-7.3	ALA175, CYS42, GLY82, GLY83, ILE85, LEU84, LEU172, TRP43	1 (GLY83 2.18Å)	9	C-H bond, Pi-Sulfur, Alkyl
21d	-7.9	ALA175, ASN173, CYS42, GLY82, GLY83, ILE85, HIS174, LEU84	1 (ASN173 2.42Å), 1 (GLY83 2.90Å), 1 (LEU172 2.42Å)	11	van der Waals, C-H bond, Unfavorable Acceptor-Acceptor, Pi-Pi Stacked, Amide-Pi Syacked, Alkyl, Pi-Alkyl

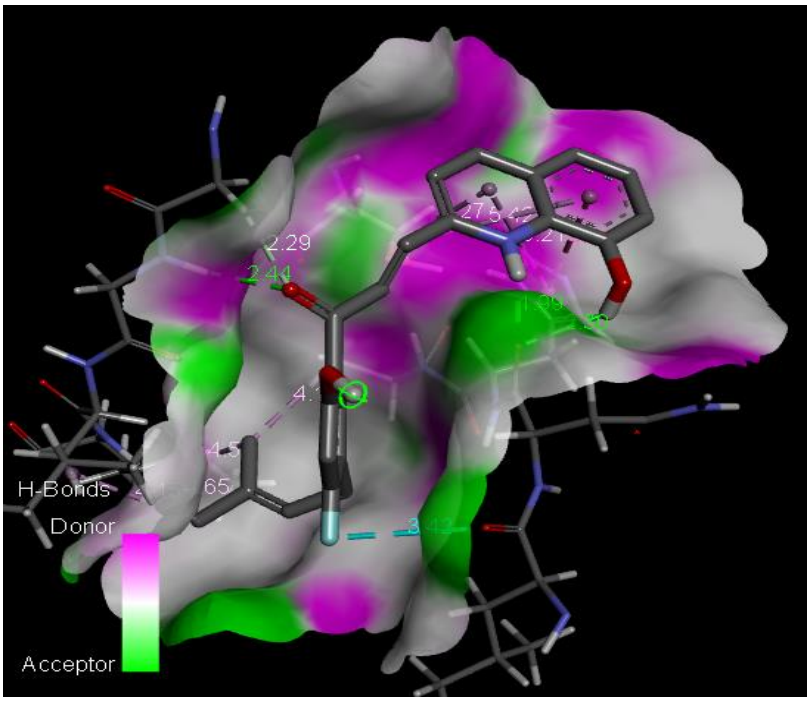

(a)

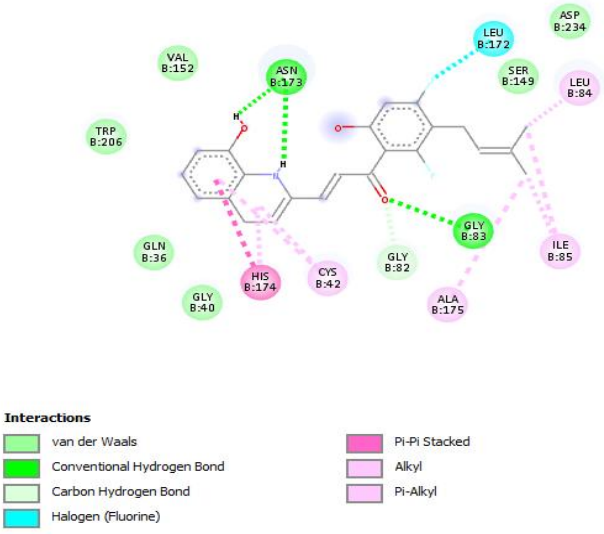

(b)

Figure 3 Binding interaction of 13d with Falcipain 2 in 3D (a) and 2D (b)

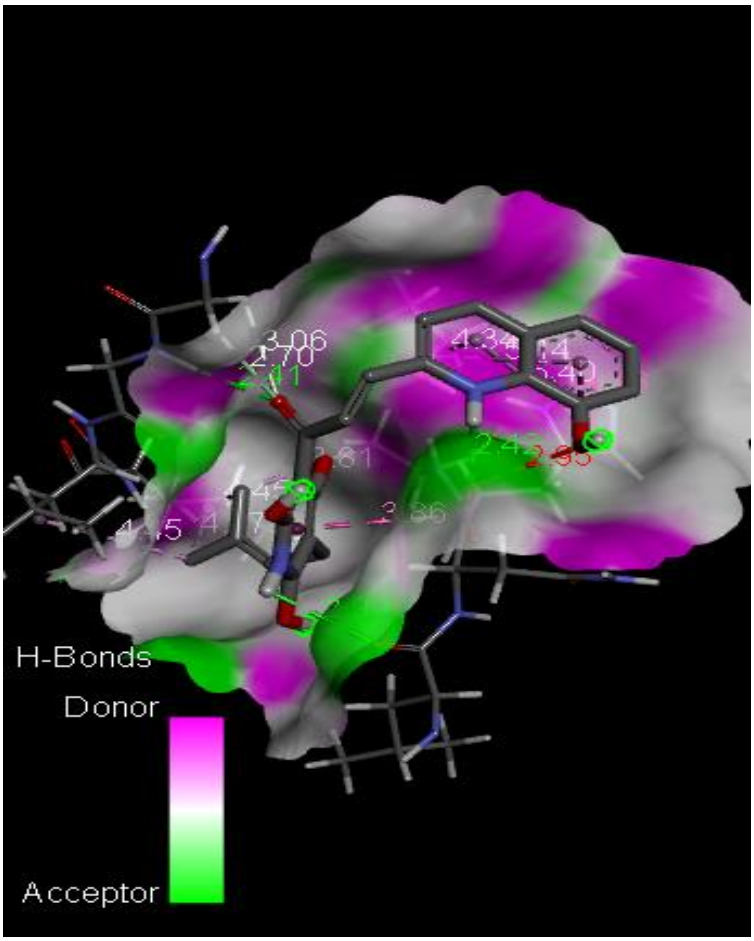

(a)

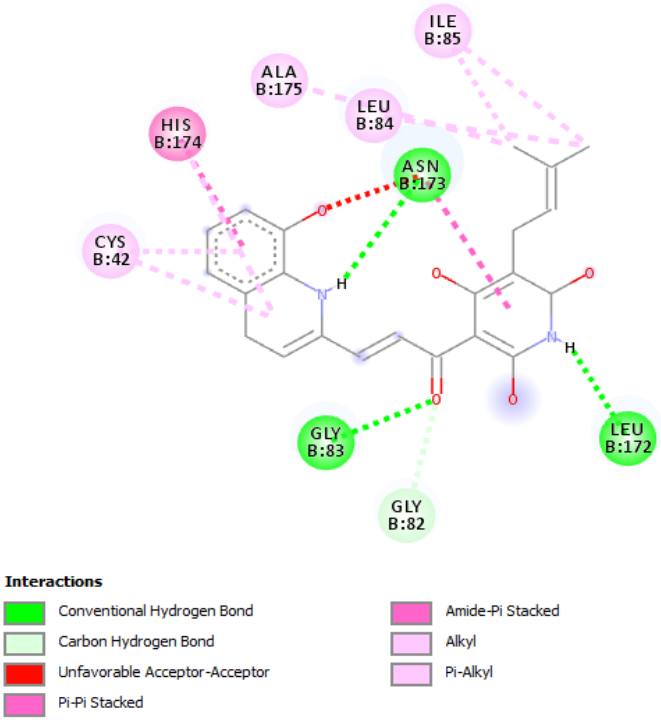

(b)

Figure 4 Binding interaction of 21d with Falcipain 2 in 3D (a) and 2D (b)

Table 10 Binding affinity analysis of the selected compounds for *Pf* Falcipain 3

Cpds	P. Falciapain 3				
	BE (ΔG)	Interacting residues	H-bond	HI	Types of Hydrophobic interaction (HI)
2a	-7.9	ALA46, ALA161, ALA166, ASN182, ASP44, PHE167, TRP215	1 (ASN182 2.11Å), 1 (ASP44 2.59Å)	6	C-H bond, Pi-Pi Stacked. Alkyl, Pi-Alkyl
4a	-8.4	ALA166, ASP44, GLY49, GLN45, TRP215	1 (GLN45 2.70Å)	5	van der Waals, C-H bond, Pi-Pi Stacked. Alkyl, Pi-Alkyl
4b	-8.8	ALA166, ASN182, GLN45, TRP215, TRP219	1 (ASN182 2.62Å), 1 (GLN45 2.76Å), 1 (TRP215 2.92Å)	3	Pi-Pi T-shaped, Alkyl, Pi-Alkyl
4d	-8.5	ALA161, ALA166, ASP44, CYS51, GLN45, TRP215	1 (ASP44 2.69Å), 1 (GLN45 2.99Å), 1 (TRP215 1.97Å)	7	van der Waals, Pi-Sigma, Pi-Pi Stacked, Alkyl, Pi-Alkyl
4e	-8.3	ALA161, ALA166, ASN182, GLN45, TRP215	1 (GLN45 2.81Å)	8	Unfavorable Acceptor-Acceptor, Pi-Pi Stacked, Alkyl, Pi-Alkyl
7c	-8.4	ALA161, ALA166, GLN45, HIS183, TRP215	1 (ALA161 2.87Å), 1 (GLN45 2.78Å), 1 (TRP215 2.26Å)	7	C-H bond, Pi-Pi Shaped, Alkyl, Pi-Alkyl
8b	-8.4	ALA46, ALA161, ALA166, CYS51, GLN45, TRP215, TRP219	1 (CYS51 2.63Å), 1 (GLN45 2.58Å), 1 (TRP215 3.08Å)	8	van der Waals, Halogen (Cl, Br, I), Pi-Sulfur, Pi-Pi Stacked, Pi-Pi T-shaped, Alkyl, Pi-Alkyl
8d	-8.5	ALA161, ALA166, CYS51, GLN45, HIS183, TRP215	1 (CYS51 2.69Å), 1 (GLN45 2.74Å)	8	Pi-Sigma, Pi-Sulfur, Pi-Pi Stacked, Pi-Pi T-shaped, Alkyl, Pi-Alkyl
8f	-8.6	ALA46, ALA161, ALA166, ASN182, TRP215, TRP219	1 (ASN182 2.65Å), 1(TRP215 3.00Å)	5	Halogen (Cl, Br, I), Pi-Pi Stacked, Pi-Pi T-shaped, Alkyl, Pi-Alkyl
10e	-7.7	ALA166, GLN45, PHE167, TRP215	1 (GLN45 2.37Å), 1 (TRP215 2.43Å)	8	Pi-Sigma, Pi-Pi Stacked, Alkyl, Pi-Alkyl
11d	-8.4	ALA161, ALA166, ASP44, CYS48, TRP215	1 (ASP44 2.81Å), 1 (CYS48 2.28Å), 1 (TRP215 2.28Å)	5	van der Waals, Pi-Pi Stacked, Amide-Pi Stacked, Alkyl, Pi-Alkyl
11e	-8.1	ALA161, ALA166, CYS48, GLN45, TRP215	1 (GLN45 2.78Å), 1 (CYS48 2.27Å)	6	van der Waals, Pi-Sigma, Pi-Pi Stacked, Amide-Pi Stacked, Alkyl, Pi-Alkyl
13a	-8.4	ALA46, ALA161, ALA166, ASN182, PHE167, TRP215	2 (ALA46 1.99Å, 2.96Å), 1 (ASN182 2.07Å)	6	C-H bond, Halogen (F), Pi-Pi Stacked, Alkyl, Pi-Alkyl
13b	-8.4	ALA161, ALA166, CYS48, TRP215	1 (CYS48 2.32Å), 1 (TRP215 2.42Å)	6	van der Waals, Pi-Pi Stacked, Amide-Pi Stacked, Alkyl, Pi-Alkyl
13d	-8.5	ALA161, ALA166, ASN182, ASP44, CYS48, CYS51, HIS183, TRP215	2 (ASP44 2.82Å, 2.87Å), 1 (CYS48 2.40Å), 1 (HIS183 2.83Å) 1 (TRP215 2.50Å)	7	C-H bond, Halogen (F), Pi-Sulfur, Pi-Pi Stacked, Alkyl, Pi-Alkyl

13e	-8.5	ALA161, ALA166, ASN182	_____	6	Halogen (F), Pi-Sigma, Pi-Pi Stacked, Alkyl, Pi-Alkyl
13f	-8.4	ALA46, ALA161, ALA166, ASN182, TRP215, TRP219	1 (TRP215 3.00Å)	6	Halogen (Cl, Br, I), Halogen (F), Pi-Pi T-shaped, Alkyl, Pi-Alkyl
15d	-8.4	ALA161, CYS48, TRP215	1 (CYS48 2.62Å), 1 (TRP215 2.19Å)	5	van der Waals, Pi-Sigma, Pi-Pi Stacked, Amide-Pi Stacked, Alkyl, Pi-Alkyl
16b	-8.4	ALA161, CYS48, TRP215	1 (CYS48 2.25Å)	5	van der Waals, Pi-Sigma, Pi-Pi Stacked, Amide-Pi Stacked, Alkyl, Pi-Alkyl
16d	-8.4	ALA161, ALA166, ASP44, CYS48, CYS89, GLY49, TRP215	1 (ASP44 2.97Å), 1 (CYS48 2.26Å)	7	van der Waals, Pi-Sigma, Pi-Pi Stacked, Amide-Pi Stacked, Alkyl, Pi-Alkyl
18d	-8.3	ALA161, ALA166, ASP44, GLN45, TRP215	1 (ASP44 3.02Å), 1 (GLN45 2.73Å), 1 (TRP215 2.71Å)	6	Pi-Sigma, Pi-Pi Stacked, Alkyl, Pi-Alkyl
19a	-8.3	ALA46, ASN182, TRP215, TRP219	1 (ALA44 2.11Å), 1 (ASN182 2.12Å)	3	van der Waals, Pi-Pi Stacked, Pi-Alkyl
19d	-8.1	ALA46, ALA166, CYS48, GLY49, TRP215, TYR90	1 (ALA46 2.30Å), 1 (TRP215 2.28Å)	6	van der Waals, Pi-Pi Stacked, Amide-Pi Stacked, Alkyl, Pi-Alkyl
21a	-8.3	ALA161, ALA166, ASN182, ASP44, HIS183, TRP215	2 (ASN182 2.86Å, 2.94Å)	10	C-H bond, Pi-Donor Hydrogen bond, Pi-Pi-Pi Stacked, Pi-Pi T-shaped, Alkyl, Pi-Alkyl
21d	-8.0	ALA161, ALA166, ASP44, CYS48, CYS51, HIS183, TRP215	1(ASP44 2.68Å), 1(CYS48 2.32Å), 1(TRP215 2.40Å)	8	Pi-Sigma, Pi-Sulfur, Pi-Pi Stacked, Pi-Pi T-shaped, Alkyl, Pi-Alkyl

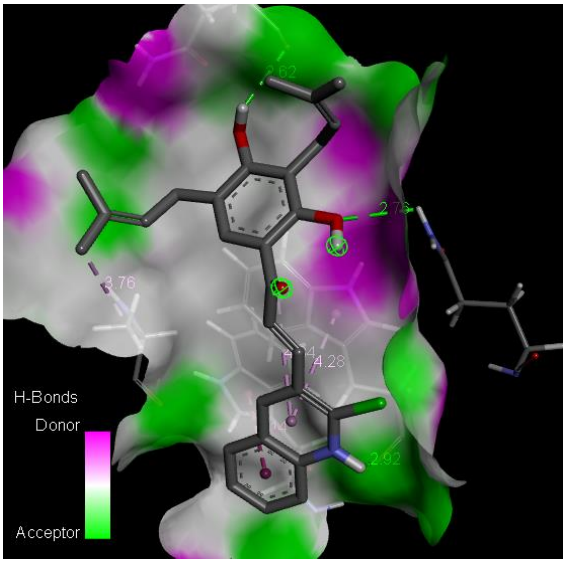

(a)

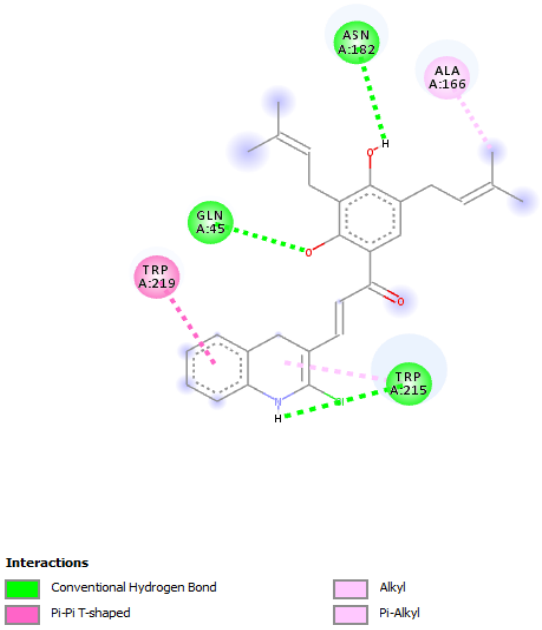

(b)

Figure 5 Binding interaction of 4b with Falcipain 3 in 3D (a) and 2D (b)

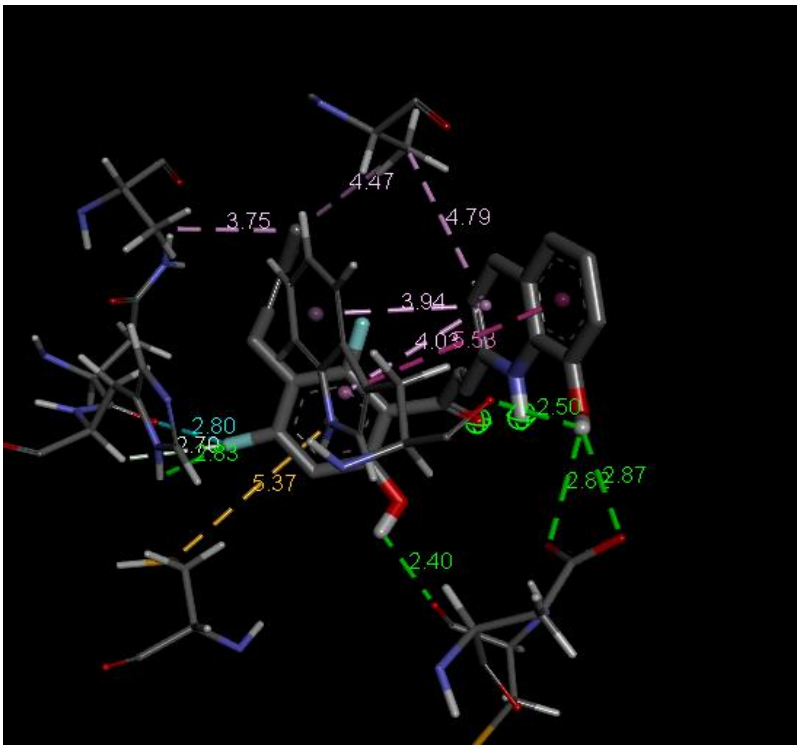

(a)

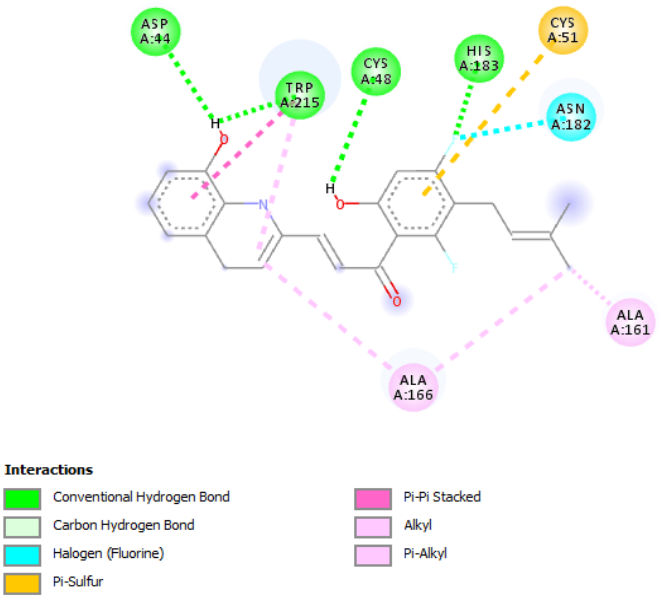

(b)

Figure 6 Binding interaction of 13d with Falcipain 3 in 3D (a) and 2D (b)

Table 11 Binding affinity analysis of the selected compounds for *Pf* SUB1

Cpds	Pf SUB1				
	BE (ΔG)	Interacting residues	H-bond	Hydophobic interaction	Types of HI
2a	-7.9	LEU466, LYS465, MET472, PHE491, SER490	1 (LYS465 2.28Å), 1 (SER490 2.12Å)	5	C-H bond, Pi-Sulfur, Alkyl, Pi-Alkyl
4a	-7.4	GLY467, LEU469, PHE493	1 (GLY467 2.72Å)	3	Alkyl, Pi-Alkyl
4b	-8.1	HIS428, LEU466, LEU469, LEU602, LYS465, MET472, PHE493, TYR427	_____	9	Pi-Pi Stacked, Alkyl, Pi-Alkyl
4d	-8.2	HIS428, LEU469, LYS465, PHE493	_____	6	Pi-Pi T-shaped, Alkyl, Pi-Alkyl
4e	-8.2	GLY467, LEU469, LYS465, PHE493	1 (GLY467 2.53Å), 1 (LYS465 2.08Å)	5	C-H bond, Alkyl, Pi-Alkyl
7c	-7.8	ARG468, ASN520, GLY467, LYS465, SER606	1 (ARG468 2.74Å), 3 (ASN520 2.53Å, 2.66Å, 2.69Å), 1 (GLY467 2.70Å), 1 (SER606 2.62Å)	5	C-H bond, Amide-Pi Stacked, Pi-Alkyl
8b	-7.9	HIS428, LEU466, LEU469, LYS465, SER490, PHE493	1 (HIS428 2.98Å), 1 (LYS465 2.48Å), 1 (SER490 2.64Å)	4	Van der Waals, Pi-Pi Stacked, Alkyl, Pi-Alkyl
8d	-7.6	LEU466, LYS465, PHE493, SER606	1 (LYS465 2.41Å)	6	C-H bond, unfavorable Donor-Donor, Pi-Pi Stacked, Alkyl, Pi-Alkyl
8f	-7.6	GLY467, HIS428, MET472, LEU469, MET472, PHE491, PHE493, SER606	1 (HIS428 2.69Å), 1 (LYS465 2.76Å), 1 (SER606 2.15Å)	7	Pi-Pi T-shaped, Alkyl, Pi-Alkyl

10e	-8.1	HIS428, LEU461, LEU469, LYS465, PHE491, PHE493	————	12	Pi-Pi Stacked, Pi-Pi T-shaped, Alkyl, Pi-Alkyl
11d	-7.4	ASN520, HIS428, LEU461, LEU466, LEU602, LYS465, SER606,	1 (ASN520 2.83Å), 1 (HIS428 2.83Å), 1(LYS465 2.01Å), 1 (SER606 2.11Å)	3	Alkyl
11e	-7.5	ASN520, HIS428, LEU466, LEU602, LYS465, SER490, SER606	1(ASN520 2.87Å), 1(HIS428 2.88Å), 1 (SER606 2.09Å)	5	C-H bond, Unfavorable Donor-Donor, Unfavorable Acceptor-Acceptor, Pi-Cation, Alkyl
13a	-8.1	GLY467, HIS428, LEU469, PHE493	1 (GLY467 2.55Å)	4	C-H bond, Pi-Pi Stacked, Pi-Pi T-shaped, Pi-Alkyl
13b	-7.9	GLY467, LEU469, PHE493, SER519	1 (GLY467 2.39Å)	4	Van der Waals, C-H bond, Pi-Donor hydrogen bond, Pi-Pi Stacked, Pi-Alkyl
13d	-8.0	GLY467, LEU469, PHE493, SER492, SER519	1 (GLY467 2.55Å)		C-H bond, Unfavorable Donor-Donor, Pi-Donor Hydrogen bond, Pi-Alkyl
13e	-8.0	GLY467, LEU469, LYS465, MET472, PHE491, PHE493	1 (GLY467 3.07Å), 1 (LYS465 2.61Å)	6	C-H bond, Alkyl, Pi-Alkyl
13f	-8.0	GLY467, LEU469, PHE493, SER606	1 (SER606 1.91Å)	4	Van der Waals, C-H bond, Halogen (F), Pi-Pi Stacked, Pi-Alkyl
15d	-7.8	ASN520, HIS428, LEU469, MET472, PHE493, SER519	1 (ASN520 2.66Å)	5	Unfavorable Donor-Donor, Pi-Pi Stacked, Alkyl, Pi-Alkyl
16b	-7.9	HIS428, LEU602, LYS465, MET472, PHE493, TYR427	1 (HIS428 2.83Å), 1 (LYS465 2.81Å)	5	C-H bond, Pi-Sulfur, Pi-Pi Stacked, Alkyl, Pi-Alkyl
16d	-7.9	ASP494, HIS428, LEU469, LYS465, PHE493, SER490	1 (SER490 2.78Å)	5	C-H bond, Pi-Pi T-shaped, Alkyl, Pi-Alkyl
18d	-7.8	GLU495, ILE499, LEU469, PHE473, PHE493	————	9	Van der Waals, Pi-Anion, Pi-Pi Stacked, Alkyl, Pi-Alkyl
19a	-7.9	GLY467, LEU466, LEU469, PHE493	1 (GLY467 2.07Å)	6	C-H bond, Pi-Pi Stacked, Alkyl, Pi-Alkyl
19d	-8.1	GLY467, LEU466, LEU469, PHE493, SER490	1 (GLY467 2.14Å), 1 (SER490 3.02Å)	6	Van der Waals, C-H bond, Unfavorable Acceptor-Acceptor Pi-Pi Stacked, Alkyl, Pi-Alkyl
21a	-7.8	HIS428, LYS465, PHE493, SER492	1 (LYS465 2.00Å), 1 (SER492 2.13Å)	2	Van der Waals, C-H bond, Pi-Pi Stacked, Pi-Alkyl
21d	-7.8	HIS428, LEU469, LYS465, MET472, PHE493, SER490	1 (SER490 2.58Å)	6	Pi-Sulfur, Pi-Pi Stacked, Alkyl, Pi-Alkyl

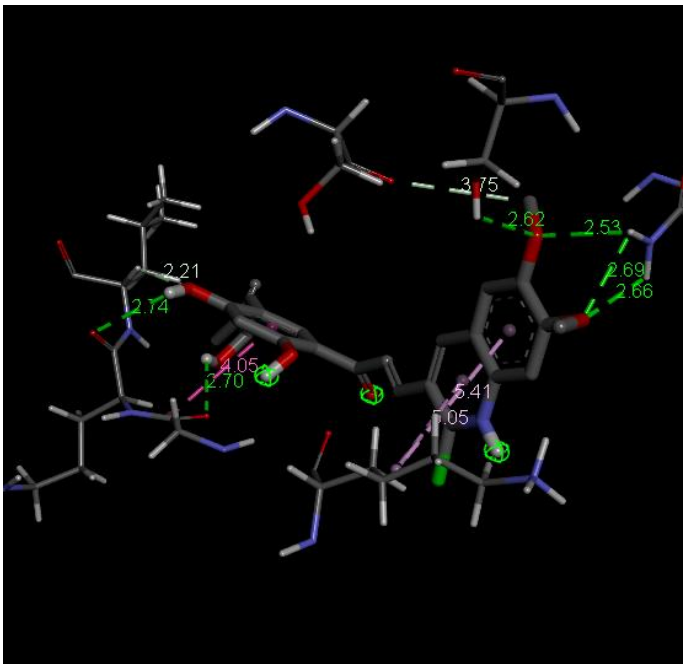

(a)

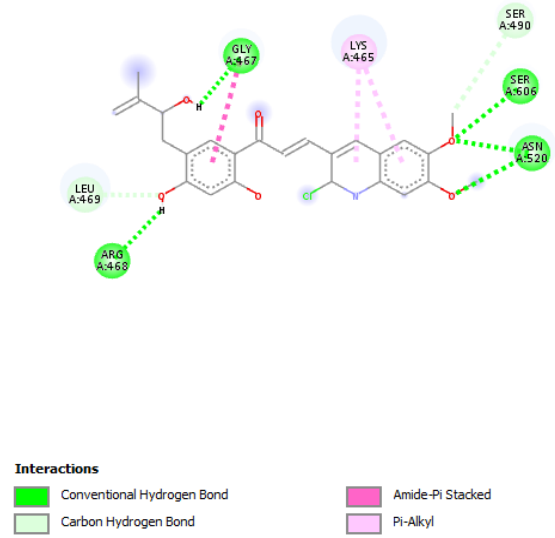

(b)

Figure 7 Binding interaction of 7c with Falcipain 3 in 3D (a) and 2D (b)

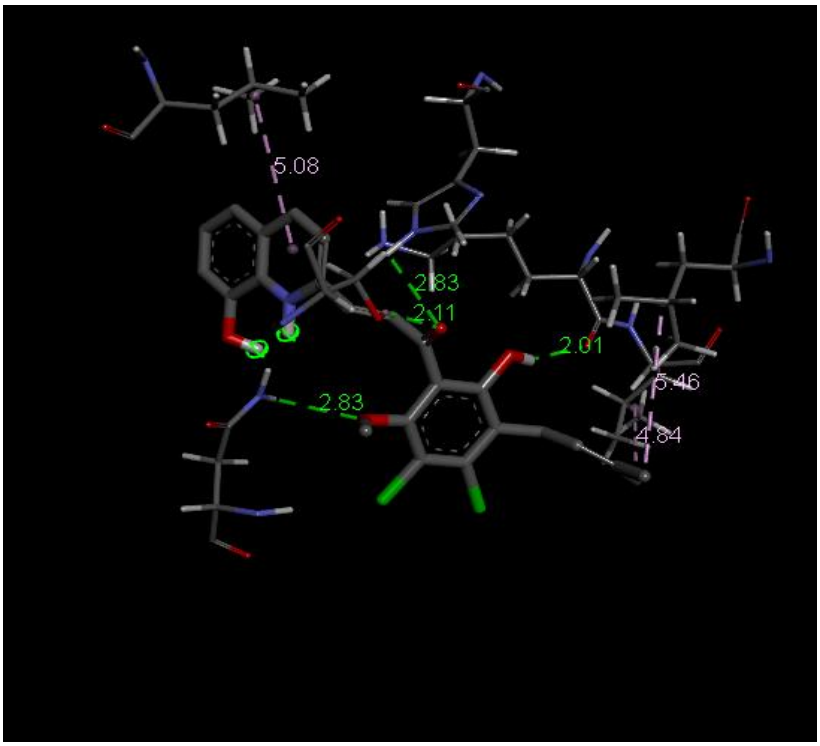

(a)

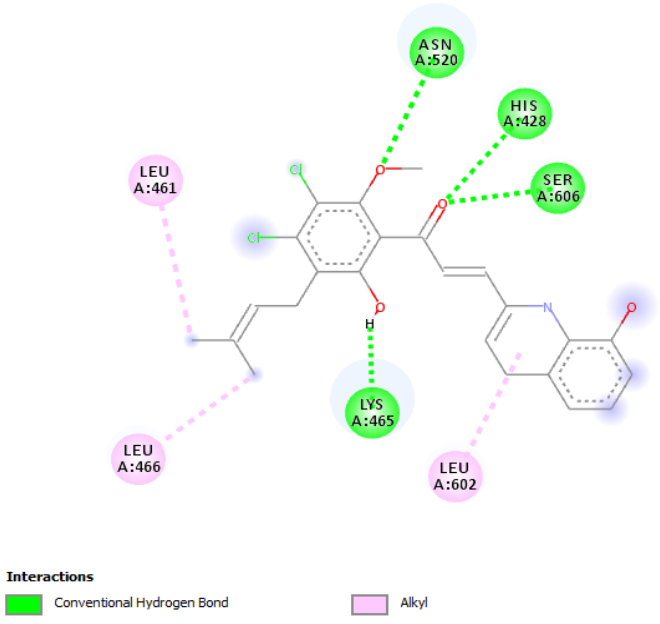

(b)

Figure 8 Binding interaction of 11d with Falcipain 3 in 3D (a) and 2D (b)

Molecular Docking Simulation

The binding interactions as viewed on Discovery studio visualizer show that all the selected compounds have good poses on the receptors (Table 8, 9, 10, 11). While compounds 19d and 21d had five and seven hydrogen bonds respectively with plasmepsin II residues in addition to other hydrophobic bonds (Figure 1, 2) which is in line with their low binding energy. Compounds 13d, 15d and 21d had three hydrogen bonds each with the Falcipain 2 residues in addition to other hydrophobic interactions (Figure 3, 4). With Falcipain 3, compounds 13d had five hydrogen bonds in addition to other hydrophobic interactions (Figure 6) whereas compounds 4b (Figure 5), 4d, 7c, 8c, 11d, 13a, 18d and 21d had three hydrogen bonds each with the receptor residues (Table 8).

Compounds 7c and 11d had six and four hydrogen bonds respectively with SUB1 residues in addition to other hydrophobic interactions (Figure 7, 8). From the molecular simulation results of the hybrids, it stems out that compounds having the quinoline fragment with additional hydroxyl group at position-8 (fragment d) shows a great binding affinity for all the receptors. This is in accordance to the (fragment d) high ranking in the fragments binding energy ranking (unpublished). This is indicating its potential as possible nucleus for new antimalarial agents.

5. CONCLUSION

Overall findings showed that selected compounds with the highest affinities for the chosen biological targets for malaria (PlmII, Falcipain 2 and 3 and SUB1) had plausible drug-able features, elevating them to the status of potential antimalarial drug candidates.

Acknowledgement

The authors acknowledge Shanghai Key Laboratory of New Drug Design, School of Pharmacy, Shanghai University of Science and Technology, East China, SwissADME and Admetlab 2.0 teams for their computational resources. We also acknowledge ChemAxxon Ltd. (www.chemaxon.com) for their free licence Marvin JS for drawing and optimization of the compounds.

Informed consent

Not applicable.

Ethical approval

Not applicable.

Conflicts of interests

The authors declare that there are no conflicts of interests.

Funding

The study has not received any external funding.

Data and materials availability

All data associated with this study are present in the paper.

REFERENCES AND NOTES

1. Agarwal S, Singh MK, Garg S, Chitnis CE, Singh S. Ca^{2+}-mediated exocytosis of subtilisin-like protease 1: A key step in egress of Plasmodium falciparum merozoites. Cell Microbiol 2012; 15:910–921.
2. Asojo OA, Gulnik SV, Afonina E, Yu B, Ellman JA, Haque TS, Silva AM. Novel uncomplexed and complexed structures of plasmepsin II, an aspartic protease from Plasmodium falciparum. J Mol Biol 2003; 327(1):173-81. doi: 10.1016/s0022-2836(03)00036-6
3. Babalola S, Igie N, Odeyemi I. Molecular Docking, Drug-Likeness Analysis, In Silico Pharmacokinetics and Toxicity Studies of p -Nitrophenyl Hydrazones as Anti-inflammatory Compounds against COX-2, 5-LOX and H /K ATPase. Pharm Front 2022; 4(4):e250-e266. doi: 10.1055/s-0042-1759688
4. Biamonte MA, Wanner J, Le-Roch KG. Recent advances in malaria drug discovery. Bioorg Med Chem Lett 2013; 23:2829.
5. Burrows JN, Duparc S, Gutteridge WE, Hooft van Huijsduijnen R, Kaszubska W, Macintyre F, Mazzuri S, Möhrle JJ, Wells TNC. New developments in anti-malarial target candidate and product profiles. Malar J 2017; 16(1):26. doi: 10.1186/s12936-016-1675-x
6. Clark DE, Pickett SD. Computational methods for the prediction of 'drug-likeness'. Drug Discov Today 2000; 5(2):49-58. doi: 10.1016/s1359-6446(99)01451-8
7. Collins CR, Hackett F, Strath M, Penzo M, Withers-Martinez C, Baker DA, Blackman MJ. Malaria parasite cGMP-dependent protein kinase regulates blood stage merozoite secretory organelle discharge and egress. PLoS Pathog 2013; 9(5):e1003344. doi: 10.1371/journal.ppat.1003344
8. Daina A, Zoete V. A BOILED-Egg to Predict Gastrointestinal Absorption and Brain Penetration of Small Molecules. ChemMedChem 2016; 11:1117–1121. doi: 10.1002/cmdc.201600182
9. Guan L, Yang H, Cai Y, Sun L, Di P, Li W, Liu G, Tang Y. ADMET-score – a comprehensive scoring function for evaluation of chemical drug-likeness. Med Chem Commun 2019; 10:148-157. doi: 10.1039/C8MD00472B

10. Jhoti H, Williams G, Rees DC, Murray CW. The rule of three for fragment-based drug discovery: Where are we now? Nat Rev Drug Discov 2013; 12:644. doi: 10.1038/nrd3926-c1
11. Kashyap A, Chetia D, Rudrapal M. Synthesis, Antimalarial Activity Evaluation and Drug likeness Study of Some New Quinoline-Lawsone Hybrids. Ind J Pharm Sci 2017; 78:801–809.
12. Kerr ID, Lee JH, Farady CJ, Marion R, Rickert M, Sajid M, Pandey KC, Caffrey CR, Legac J, Hansell E, Mc-Kerrow JH, Craik CS, Rosenthal PJ, Brinen LS. Vinyl sulfones as antiparasitic agents and a structural basis for drug design. J Biol Chem 2009; 284(38):25697-703. doi: 10.1074/jbc.M109.014340
13. Klein EY. Antimalarial drug resistance: A review of the biology and strategies to delay emergence and spread. Int J Antimicrob Agents 2013; 41(4):311-7. doi: 10.1016/j.ijantimicag.2012.12.007
14. Kola I, Landis J. Can the pharmaceutical industry reduce attrition rates? Nat Rev Drug Discov 2004; 3(8):711-5. doi: 10.1038/nrd1470
15. Koussis K, Withers-Martinez C, Yeoh S, Child M, Hackett F, Knuepfer E, Juliano L, Woehlbier U, Bujard H, Blackman MJ. A multifunctional serine protease primes the malaria parasite for red blood cell invasion. EMBO J 2009; 28(6):725-35. doi: 10.1038/emboj.2009.22
16. Liu X, Wright M, Hop CE. Rational use of plasma protein and tissue binding data in drug design. J Med Chem 2014; 57(20):8238-48. doi: 10.1021/jm5007935
17. Mansoor A, Mahabadi N. Volume of Distribution. In: Stat Pearls (Internet) 2021.
18. Menezes CMS, Sant'Anna CMR, Rodrigues CR, Barreiro EJ. Molecular modeling of novel 1H-pyrazolo (3, 4-b) pyridine derivatives designed as isosters of the antimalarial mefloquine. J Mol Struct 2002; 579:31-9.
19. Meunier B. In: Polypharmacology in Drug Discovery, Peters JU (Ed), John Wiley & Sons, Inc 2012.
20. Mullard A. 2017 FDA drug approvals. Nat Rev Drug Discov 2018; 17(2):81-85. doi: 10.1038/nrd.2018.4
21. Muregi FW, Ishih A. Next-Generation Antimalarial Drugs: Hybrid Molecules as a New Strategy in Drug Design. Drug Dev Res 2010; 71(1):20-32. doi: 10.1002/ddr.20345
22. Muregi FW, Kirira PG, Ishih A. Novel rational drug design strategies with potential to revolutionize malaria chemotherapy. Curr Med Chem 2011; 18(1):113-43. doi: 10.2174/092986711793979742
23. Phyo AP, Jittamala P, Nosten FH, Pukrittayakamee S, Imwong M, White NJ, Duparc S, Macintyre F, Baker M, Möhrle JJ. Antimalarial activity of artefenomel (OZ439), a novel synthetic antimalarial endoperoxide, in patients with Plasmodium falciparum and Plasmodium vivax malaria: An open-label phase 2 trial. Lancet Infect Dis 2016; 16(1):61-69. doi: 10.1016/S1473-3099(15)00320-5
24. Robertson S, Penzak S, Huang S. Principles of clinical pharmacology. Third edition 2012; 239-257. doi: 10.1016/B978-0-12-385471-1.00015.5
25. Ruecker A, Shea M, Hackett F, Suarez C, Hirst EM, Milutinovic K, Withers-Martinez C, Blackman MJ. Proteolytic activation of the essential parasitophorous vacuole cysteine protease SERA6 accompanies malaria parasite egress from its host erythrocyte. J Biol Chem 2012; 287(45):37949-63. doi: 10.1074/jbc.M112.400820
26. Schlitzer M. Antimalarial Drugs – What is in Use and what is in the Pipeline. Arch Pharm Life Sci 2008; 341:149.
27. Siezen RJ, Leunissen JA. Subtilases: The superfamily of subtilisin-like serine proteases. Protein Sci 1997; 6(3):501-23. doi: 10.1002/pro.5560060301
28. Sinha S, Batovska DI, Medhi B, Radotra BD, Bhalla A, Markova N, Sehgal R. In vitro anti-malarial efficacy of chalcones: cytotoxicity profile, mechanism of action and their effect on erythrocytes. Malar J 2019; 18:421.
29. Siramshetty VB, Nickel J, Omieczynski C, Gohlke BO, Drwal MN, Preissner R. WITHDRAWN-a resource for withdrawn and discontinued drugs. Nucleic Acids Res 2016; 44(D1):D1080-6. doi: 10.1093/nar/gkv1192
30. Thomas JA, Tan MYS, Bisson C, Borg A, Umrekar T, Hackett F, Hale V, Vizcay-Barrena G, Fleck R, Snijders A, Saibil H, Blackman M. Publisher Correction: A protease cascade regulates release of the human malaria parasite Plasmodium falciparum from host red blood cells. Nat Microbiol 2018. doi: 10.1038/s41564-018-0111-0
31. Trott O, Olson AJ. AutoDock Vina: Improving the speed and accuracy of docking with a new scoring function, efficient optimization and multithreading. J Comput Chem 2010; 31(2):455-61. doi: 10.1002/jcc.21334
32. Veber DF, Johnson SR, Cheng HY, Smith BR, Ward KW, Kopple KD. Molecular properties that influence the oral bioavailability of drug candidates. J Med Chem 2002; 45(12):2615-23. doi: 10.1021/jm020017n
33. Walsh JJ, Bell A. Hybrid drugs for malaria. Curr Pharm Des 2009; 15:2970–2985.
34. White NJ, Duong TT, Uthaisin C, Nosten F, Phyo AP, Hanboonkunupakarn B, Pukrittayakamee S, Jittamala P, Chuthasmit K, Cheung MS, Feng Y, Li R, Magnusson B, Sultan M, Wieser D, Xun X, Zhao R, Diagana TT, Pertel P, Leong FJ. Antimalarial Activity of KAF156 in Falciparum and Vivax Malaria. N Engl J Med 2016; 375(12):1152-60. doi: 10.1056/NEJMoa1602250
35. White NJ, Duong TT, Uthaisin C, Nosten F, Phyo AP, Hanboonkunupakarn B, Pukrittayakamee S, Jittamala P, Chuthasmit K, Cheung MS, Feng Y, Li R, Magnusson B,

Sultan M, Wieser D, Xun X, Zhao R, Diagana TT, Pertel P, Leong FJ. Antimalarial Activity of KAF156 in Falciparum and Vivax Malaria. N Engl J Med 2016; 375(12):1152-60. doi: 10.1056/NEJMoa1602250

36. White NJ, Pukrittayakamee S, Phyo AP, Rueangweerayut R, Nosten F, Jittamala P, Jeeyapant A, Jain JP, Lefèvre G, Li R, Magnusson B, Diagana TT, Leong FJ. Spiroindolone KAE609 for falciparum and vivax malaria. N Engl J Med 2014; 371(5):403-10. doi: 10.1056/NEJMoa1315860
37. WHO malaria report 2023.
38. Withers-Martinez C, Strath M, Hackett F, Haire LF, Howell SA, Walker PA, Christodoulou E, Dodson GG, Blackman MJ. The malaria parasite egress protease SUB1 is a calcium-dependent redox switch subtilisin. Nat Commun 2014; 5:3726. doi: 10.1038/ncomms4726
39. Yahya MH, Babalola SA, Idris AY, Hamza AN, Igie N, Odeyemi I, Musa AM, Olorukooba AB. Therapeutic Potency of Mono- and Diprenylated Acetophenones: A Case Study of In-Vivo Antimalarial Evaluation. Pharm Front 2023; 5(5). doi: 10.1055/s-0043-1764210
40. Yeoh S, O'Donnell RA, Koussis K, Dluzewski AR, Ansell KH, Osborne SA, Hackett F, Withers-Martinez C, Mitchell GH, Bannister LH, Bryans JS, Kettleborough CA, Blackman MJ. Subcellular discharge of a serine protease mediates release of invasive malaria parasites from host erythrocytes. Cell 2007; 131(6):1072-83. doi: 10.1016/j.cell.2007.10.049